

#313

THE MEASUREMENT OF WIND PRESSURES ON TWO-STOREY HOUSES AT AYLESBURY*

K.J. EATON and J.R. MAYNE

*Building Research Establishment, Building Research Station, Garston, Watford, Herts.
WD2 7JR (Gt. Britain)*

(Received August 2, 1974)

Summary

An account is given of the measurement of wind pressures on a two-storey housing estate on the outskirts of Aylesbury, 65 km north-west of London. The estate immediately adjoins an open country fetch extending uninterruptedly for about 15 km to the south-west. The site and installation are described, including the variable geometry building erected on open ground adjoining the estate.

Wind pressures were recorded at a total of 44 positions on seven houses in the estate, and at 72 positions on the experimental building, transducers being mounted on both walls and roofs. Load cells were also installed in the experimental building to record separately total overall loads and total roof loads. Measurements of velocity were made using cup anemometers mounted at 3 m, 5 m, and 10 m, on a fixed mast, suitably sited in the vicinity of the experimental building. In addition, anemometers mounted on a 20 m portable mast were used to investigate the upstream velocity profiles, and also the flow patterns within the urban area.

The experimental building housed all the recording equipment which comprised multichannel FM magnetic tape recorders. Records were taken in analogue form and were subsequently digitised in order to calculate mean, rms and extreme values, probability distributions, autocorrelations, power spectra and cross-correlations. Measurements have been made for a variety of wind speeds and directions, and also for several roof pitches on the experimental building between 5° and 45°. Preliminary results are presented and discussed.

1. Introduction

The majority of full-scale wind pressure measurements have been made on tall buildings and on specialised structures such as chimneys, cooling towers and bridges. One such programme of measurement on tall buildings in Central London was carried out by the Building Research Station between 1962 and 1969 and has been reported [1-7]. At the conclusion of the tall-building work, it was decided to begin a new project to measure wind pressures on low-rise buildings. There were several reasons for this decision. Firstly, the

* Paper presented at the Symposium on Full-Scale Measurements of Wind Effects on Tall Buildings and Other Structures, University of Western Ontario, 23-29 June 1974.

majority of structures in the United Kingdom are low-rise. Consequently, it is not surprising that a survey of wind damage in the United Kingdom conducted by BRS for the period 1962–1969 revealed, among other things, that a very substantial proportion of the cost of repair is incurred on low-rise structures [8]. Secondly, all these buildings are entirely immersed in the bottom 10 m of the atmospheric boundary layer. Except for a few cases of isolated dwellings with abnormal exposure, these buildings will be in the roughness layer in which the Meteorological Office makes no measurements of wind velocity, and consequently there is a very great lack of data on wind flow in this layer. Thirdly, in the latest revision of the British Standard Code of Practice [9], while the calculation of wind pressures above 10 m is based upon well known power-law velocity profiles, below 10 m it is based, not upon any measurements, but upon arbitrary linear interpolation. As there were no full-scale measurements of the effect of buildings on each other, and no systematic means of estimating shelter effects, the present project was initiated to make good these deficiencies.

This paper starts, in Section 2, with a description of the site and the houses in the estate selected for the investigation. Details of an associated experimental building are given in Section 3. Section 4 outlines the positioning of the pressure transducers, and gives details of the cabling and the reference pressure system. Velocity measurements are described in Section 5, whilst Section 6 describes the recording equipment and the methods of calibration, processing and analysis. Finally, Section 7 contains an appraisal of some of the initial results of this work, including comments on the velocity measurements, mean and extreme pressure values, pressure coefficients on both the walls and roof of the experimental building as well as on the estate houses, and spectra of both velocity and pressure measurements.

2. Site

The site chosen was on the south-west outskirts of Aylesbury, which is a town with a population of about 40,000 situated 65 km north-west of London. A plan of the site is shown in Fig.1. The estate comprises 93 two-storey houses arranged in several parallel terraces on level ground. The axis of the terraces is 28° west of north. The characteristics which led to the selection of this particular site were:

(i) The open fetch of farmland to the south-west which extends, with very few interruptions, across the vale of Aylesbury for about 15 km in gentle undulations nowhere greater than about 20 m in height. This long fetch of constant terrain, shown in Fig.3, was upstream of the estate for the prevailing wind direction so that the incident wind profile would be well defined and could be contrasted with conditions for winds blowing in the opposite direction over the urban terrain shown in Fig.4.

(ii) Immediately to the west of the estate there was open, level ground which was available for the erection of an experimental building, which could

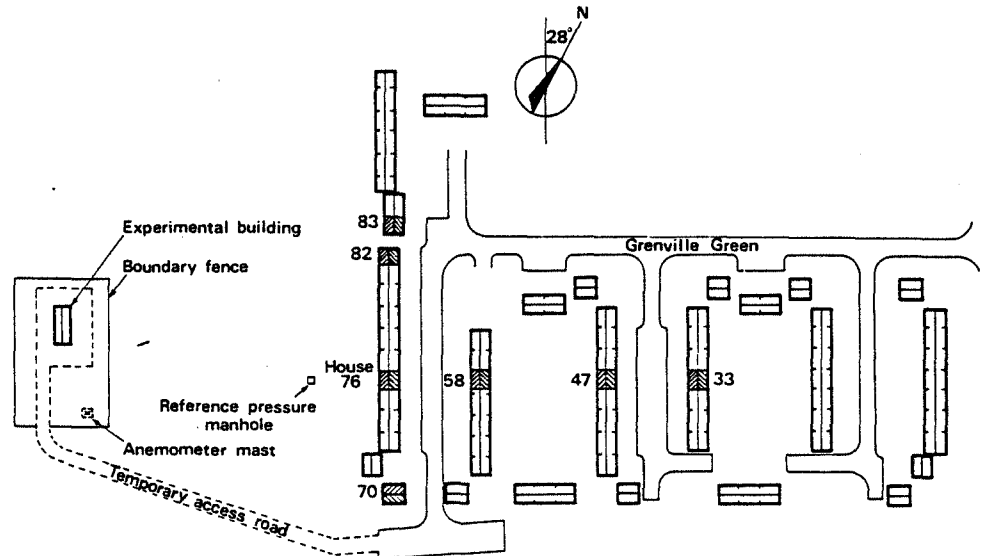


Fig.1. Plan of Aylesbury site.

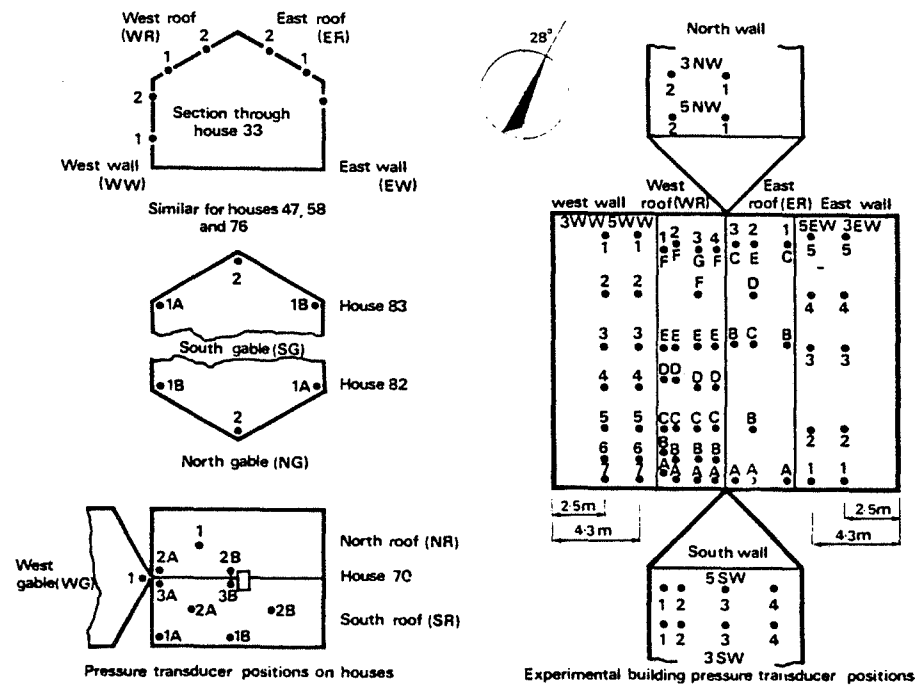


Fig.2. Position of pressure transducers on houses in the estate and on the experimental building.



Fig.3. Aylesbury site looking west.

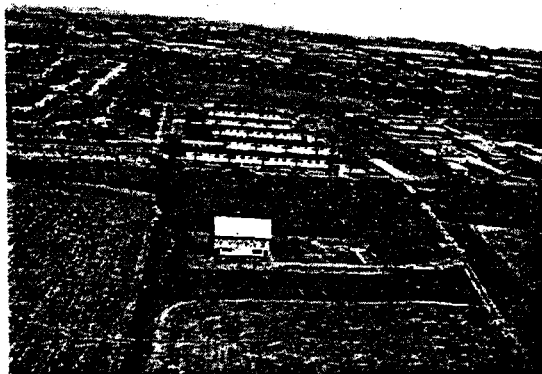


Fig.4. Aylesbury site looking east.



Fig.5. Houses in the estate.

thus be placed upstream of the estate in the prevailing wind and in a flow unobstructed by the estate from all wind directions except those between north-east and south-east. Comparison of the results from this building with those from the houses in the estate would allow assessment of the effects of shelter and varying building geometry.

(iii) The layout of the estate was simple, which would help the analysis and interpretation of the results.

A terrace of houses is shown in Fig.5. The construction was of brick load-bearing walls dividing each pair of houses in the terraces, and longitudinal external walls of cladding fixed to timber frames. The roofs were concrete-tiled with a pitch of $22\frac{1}{2}^\circ$.

3. Experimental building

The experimental building was erected to the west of the estate 100 m from the nearest houses. The position is marked on the site plan (Fig.1), and the building is shown in Figs.6–10. It was designed to fulfil the dual requirements of housing the recording equipment in a suitable and secure environment, and of providing the maximum test data for comparison with the measurements obtained from the houses in the estate. The external dimensions of the building were made identical to a pair of houses in the estate (7 m X 13.3 m) and the orientation was parallel to the axis of the terraces of the estate.

Figure 9 shows the essentials of the design. The building was of steel frame construction with six stanchions, each standing on a load cell mounted on a pile cap. Timber cladding units were fixed to the frame, and so as to ensure that all the wall loads were transferred to the frame and thence to the load cells, the bottom edge of the cladding was about 50 mm above the foundation upstand, this gap being sealed by a flexible canvas membrane. Two single-storey internal rooms, quite separate from the frame, stood directly on the foundation slab. These were thermally insulated and housed the recording equipment and amenities. The steel roof was designed to be of variable pitch between 5° and 45° . It comprised a peripheral steel sub-frame, which is shown in Figs.9 and 10, supported on the six stanchions through six additional load cells. A detail of the mounting of one of these load cells is shown in Fig.11. Each half of the roof was divided into two parts; the top parts were pinned to each other at the ridge and slid over the bottom parts which were pinned to the sub-frame at the eaves, the movement being aided by wheels fitted into telescopic rafters. Eight screw-jacks, which can be seen in Fig.10, were driven by one motor and were mounted on the sub-frame; these moved the upper parts of the roof. The gable ends were sealed at all roof pitches by a series of interleaved hanging box sections.

Figures 6, 7 and 8 show the building at various roof elevations. These figures also show shutters which were fitted in the walls and roof. The shutters were manually operated, and enabled the permeability of various parts of the building to be changed in order to investigate the influence of permeability upon internal pressure and overall forces.

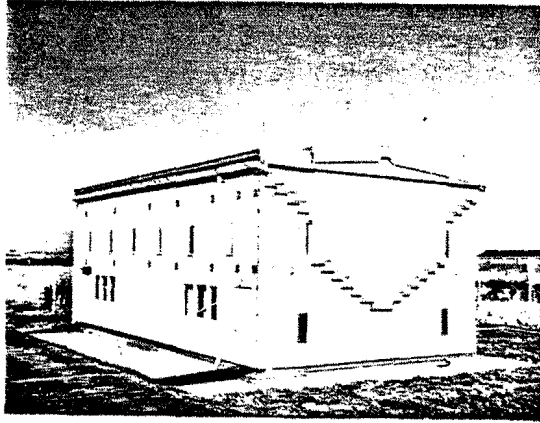


Fig. 6. Experimental building with 5° roof pitch.

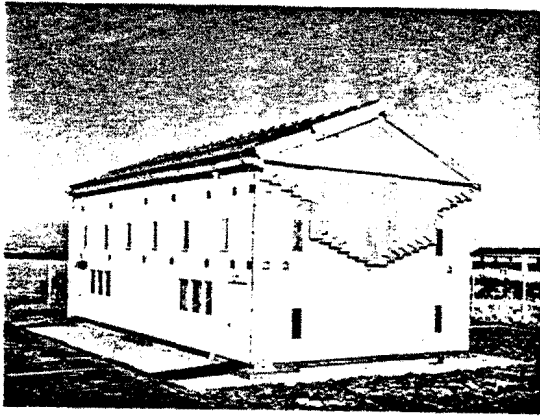


Fig. 7. Experimental building with 22½° roof pitch.

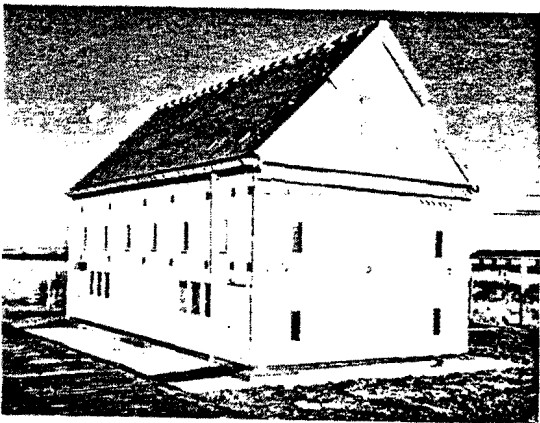


Fig. 8. Experimental building with 45° roof pitch.

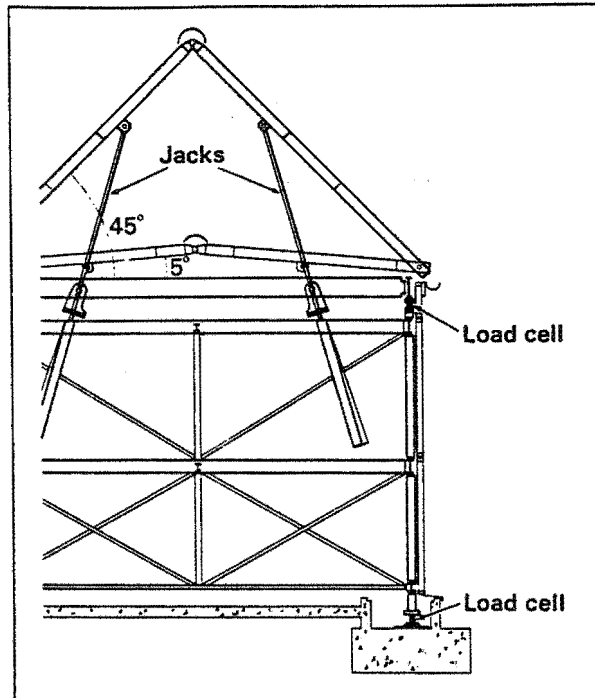


Fig.9. Experimental building showing essentials of the structure.

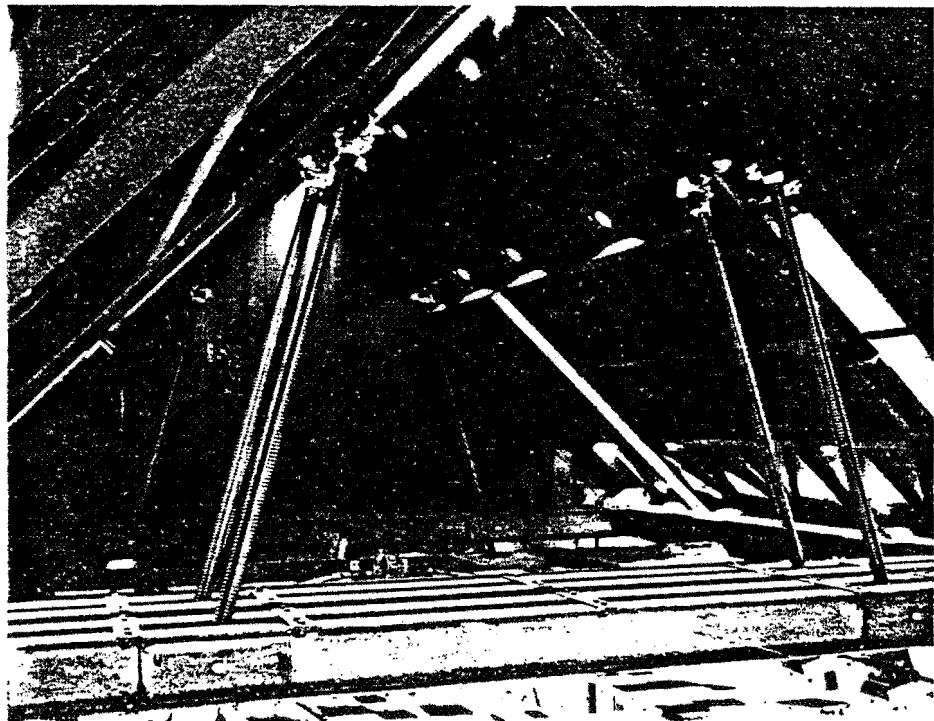


Fig.10. The interior of the roof of the experimental building during trial erection.

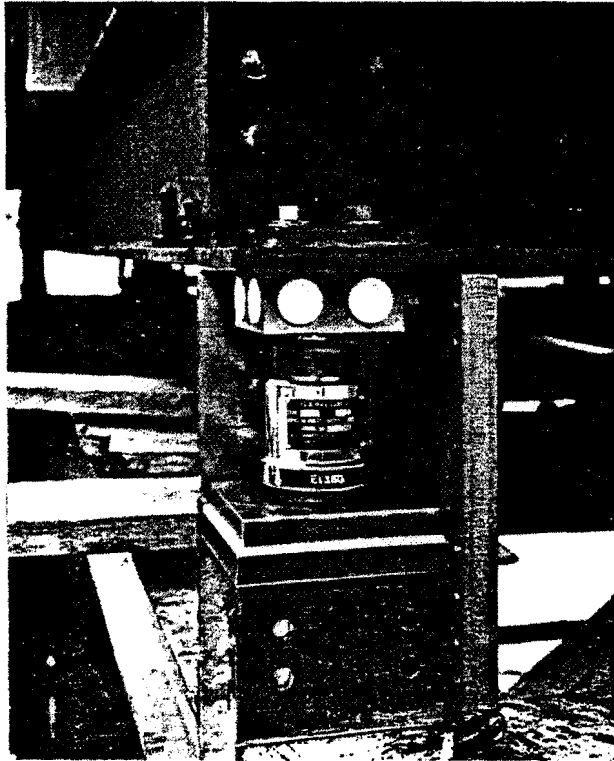


Fig.11. Detail of mounting of roof load cell.



Fig.12. Transducers mounted on the roof of house 70.

4. Pressure measurements

Transducers

The pressure transducers used were of the type developed at the Building Research Station and already described in the literature [10]. The sensitive element of these transducers consisted of a 100-mm-diameter external pressure plate mounted flush with the building surface. Figures 1 and 2 show the arrangement of these transducers. The houses in the estate were fitted with 44 transducers; 25 of these were in the roofs and 19 in the walls. For roof mounting, special tiles which were manufactured from glass-reinforced cement replaced two existing concrete tiles (Fig.12). Wall mounting was accomplished by bricking a teak box into the outer leaf of the external wall, and mounting the transducer on a metal plate screwed to the box (Fig.13).

One house was selected from the middle of each of the four most western terraces of the estate (Fig.1); seven transducers were fitted in each house in both the walls and roofs, so as to provide a complete scan of an east-west section through the estate. In addition, transducers were fitted to the gable ends of houses 82 and 83, which were separated by a narrow alleyway (3.3 m wide), in order to measure the high suctions expected in that position for certain wind directions. Transducers were also fitted in the roof of house 70 as this house was exposed to quartering winds on the south-west corner of the estate.

On the experimental building, 72 transducer sites were provided, 36 on the walls and 36 on the roof. The transducers were concentrated towards the south-west corner of the building, facing the prevailing wind. As there were only 100 transducers available, not all the positions on both houses and experimental building could be filled at any one time.

In the tall building work from 1962 to 1969, zero readings of the transducers could only be obtained during calm periods. In this project, a new provision was made for obtaining a zero reading in windy conditions. This consisted of a small hole, or zeroing port, placed in the mounting plate immediately adjacent to each transducer; this hole can be seen towards the top left-hand corner of the plate in Fig.13. Tubes connected this port, the reference venting system and the interior of the transducer to a mains-operated solenoid valve. In the unenergised state the solenoid valve connected the transducer to the venting system in the normal way and the zeroing port was disconnected. When energised, however, the venting system was disconnected and the transducer was connected to the zeroing port, thus effectively connecting the inside of the transducer to the outside. Control equipment operated the solenoid automatically at the start of every record.

Cables

Each transducer was connected to the recording apparatus in the experimental building by a single length of 4-core screened cable. These cables ran from the transducers through ducts placed in the cavity walls of the houses and in the



Fig.13. Wall-mounted transducer.

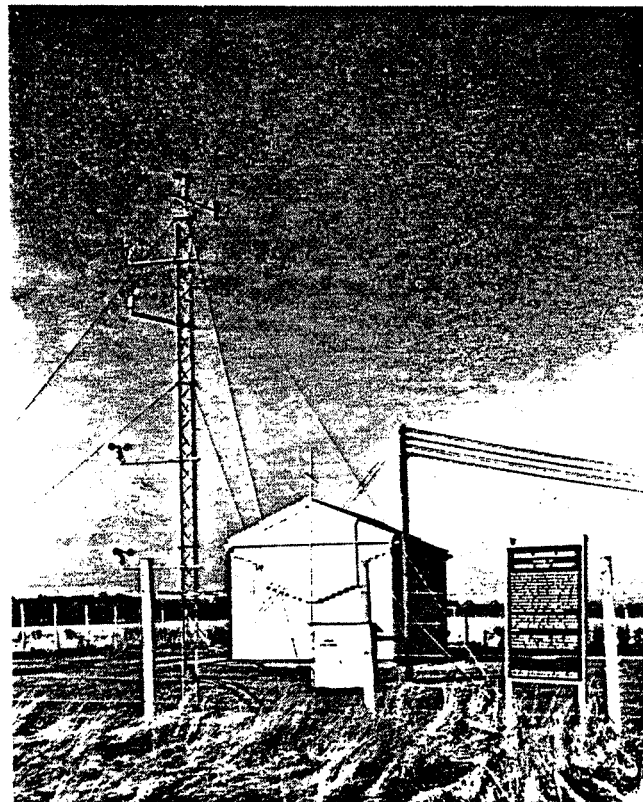


Fig.14. Anemometer mast with experimental building in background.



Fig.15. Mobile wind speed unit.

ground. In this way, the cables were protected from damage, and in most cases also kept dry, although this was not absolutely essential and some ducts subsequently filled with water without affecting the signals. Altogether 10 km of cable was installed; this was the total length of the 44 cables and, apart from 5, they required no capacitive trimming additional to that provided as standard on the signal conditioning equipment. Subsequently, two additional channels have shown drifts of capacity which required trimming. All the other channels have behaved perfectly in this respect. The cable has a capacity between adjacent conductors of up to 70,000 pF on the longest runs (400 m) which shunts the strain-gauge bridge on the transducer. By calibrating the system through the cable with the transducers *in situ*, the application of any correction was unnecessary. Similar corrections for the resistance of the cables were also thereby avoided.

Reference pressure

Venting tubes of 5-mm bore were run from each house in the same ducts as the cables and were terminated in the reference pressure manhole (Fig.1). This manhole was provided with a lid sealed except for a 25-mm-diameter hole in the centre. The manhole lid was flush with the ground at this point and the grass nearby was kept fairly short so that the hole acted as a vent to static atmospheric pressure. Transducers mounted in the experimental building could also be vented to this point giving a common reference for the entire experiment. Towards the latter stages of the project, the manhole

reference pressure was checked by comparison with a static probe mounted on the anemometer mast. The probe was to the same design as that used by Dr. R.D. Marshall at the National Bureau of Standards, Washington DC. The comparison with the manhole reference pressure showed that the mean pressure in the manhole was slightly below that of the static probe, the difference being about -0.08 times the 10 m velocity pressure.

5. Velocity measurements

About 30 m to the south-east of the building, a 10-m mast was erected (Fig.14) on which were placed three standard Meteorological Office cup anemometers at heights of 3 m, 5 m and 10 m. Direction was also measured, at 10 m only. Additionally, a Spembley "Porton" cup anemometer, which has a faster response than the standard cup anemometer, was mounted at about 9 m above the ground. These instruments were connected to the experimental building by cables and the signals were recorded simultaneously with measurements of pressures and loads. A further anemometer on the same mast was used as a wind switch to start the recording apparatus automatically in windy periods.

Mobile velocity measurements

With the dual object of obtaining more information on wind flow in urban environments and of enlarging the scope of the application of results from the Aylesbury experiments, a mobile wind speed measuring unit was set up. This comprised a Land Rover fitted with a telescopic mast of maximum height 20 m together with other portable masts which could be erected easily on site (see Fig.15). Casella "Sheppard type" cup anemometers were used, and measurements have been taken, not only at Aylesbury but also at other sites in south-east England, to investigate the effect of the layout of estates on the wind flow. This work is continuing and will be reported elsewhere. The mobile unit was used to investigate the velocity profile incident on the estate at Aylesbury from the open country fetch, and in particular to determine the effect of a 5-m-high hedge, 120 m upstream of the building, by making a measurement traverse as shown in Fig.17.

6. Data acquisition and analysis

Recording equipment

The signal conditioning equipment used for the pressure transducers and load cells consisted of 3 kHz, 5 V carrier-amplifiers manufactured by S.E. Laboratories. The outputs of these amplifiers were applied directly to eight FM magnetic tape recorders (Racal-Thermionic). Fourteen tracks were available on each recorder and 12 of these were used to record signals from transducers. One of the spare tracks on each deck was used to record a multiplexed clock pulse running at 32 pulses per second, which, during analysis of the tapes,

triggered the digitising process and allowed cross-correlations to be computed between tracks on different tapes. The other spare track recorded a fixed voltage which could be used as "flutter compensation" to reduce noise on replay. This facility was not, in fact, used, but analysis of this track permitted an assessment of the performance of the tape transports.

An ancillary control unit, built at BRS, provided the following facilities:

- (i) Automatic recording for pre-set periods when the wind speed exceeded pre-set thresholds.
- (ii) Multiplexing of the clock pulse.
- (iii) Recording of the epoch of each record by a print-out of day and time.
- (iv) Control of the initial starting sequence which consisted of activating the solenoid valves to provide zero levels and of applying standard calibration pulses as described below.
- (v) Manual operation of the whole system.

Calibration

Calibration was carried out in two parts. First an *in situ* calibration was carried out at regular intervals by applying a known deadweight load to each transducer, and the gain of the signal conditioning equipment was adjusted to maintain a standard voltage level at the input to the FM recorder. The second part of the calibration consisted of automatically applying standard ± 0.500 V signals to the FM recorders at the start of each record. As mentioned earlier, the solenoid valves were also operated at this time, providing a short period of zero values. This prelude to each record was digitised at the analysis stage and used to apply appropriate calibration factors.

Processing and analysis

The digitisation and analysis of data was carried out by the Environmental Sciences Research Unit of the Cranfield Institute of Technology who provided a rapid service of data reduction, releasing the analogue tapes for further recording in a short space of time. The analogue records were digitised at 1/32-second intervals, linear trends were removed and the data were analysed for mean, rms, maxima and minima, and percentiles of distribution. After applying digital filtering techniques, probability density functions, power spectra, autocorrelations and cross-correlations were also computed. Digital data have been stored on magnetic tapes and this will allow further computations to be made as necessary.

7. Results

Figure 16 shows the mean wind direction and maximum 2-second velocity for all the recordings which have so far been analysed. Only a selection of this material is presented in this paper. Table 1 (p.97) gives details of the records discussed.

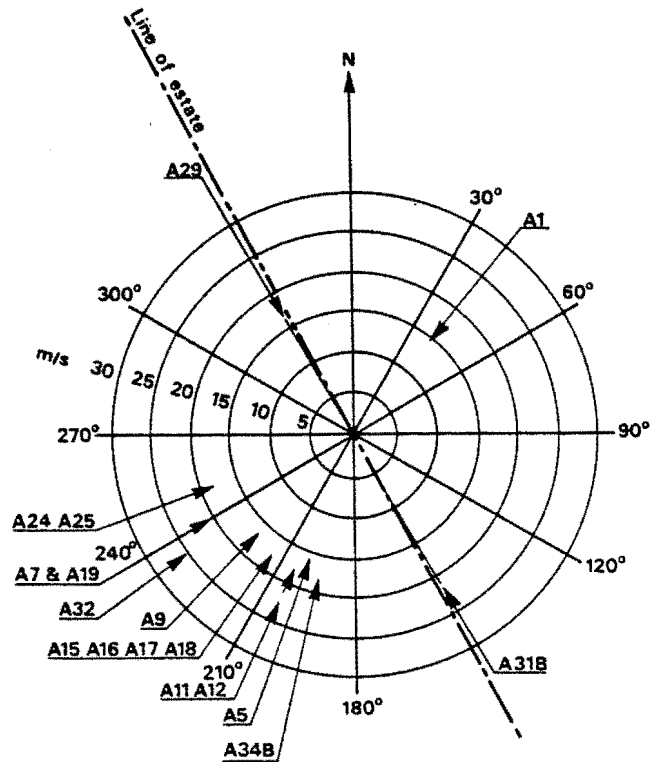


Fig.16. Mean direction and maximum wind speed for records taken at Aylesbury.

Anemometer positions across fields

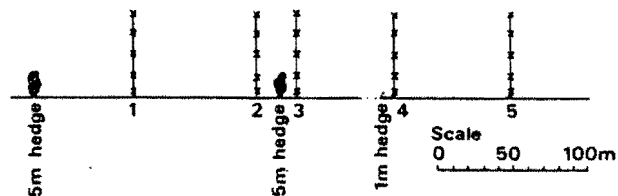
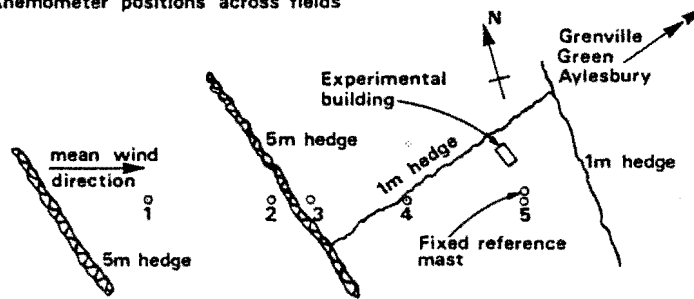


Fig.17. Velocity profile measurement points west of the estate.

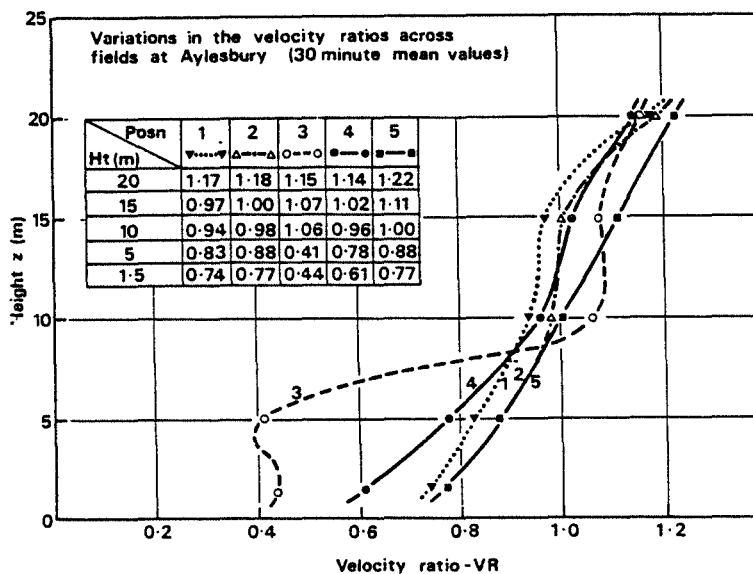


Fig.18. Velocity profiles west of the estate.

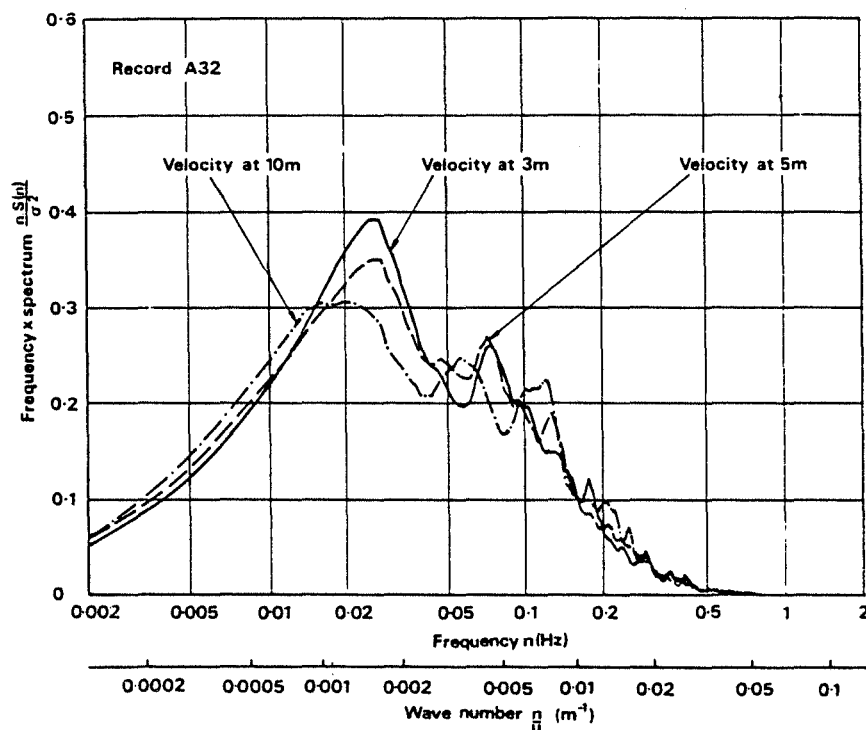


Fig.19. Comparison of velocity spectra at 3, 5 and 10 m.

Velocity measurements

Velocity measurements were made to the west of the estate. The object of these measurements was to determine whether the effect of the hedges extended as far as the experimental building and the fixed anemometer mast, and if so to what degree. The positions of the portable mast used in the measurements are shown in Fig.17. In Fig.18, the results are presented as velocity ratios, defined at any given position and height for a given averaging period as:

$$VR = \frac{\text{the maximum velocity at that position and height for that averaging period}}{\text{the maximum velocity at 10 m on the reference mast for the same averaging period}}$$

The velocity deficit in the lowest 5 m caused by the hedge just upstream of position 3 (Fig.17) is very apparent. At position 4 this effect still shows slightly at 5 m, while at 1.5 m the effect of the 1 m hedge is also apparent. At 10 m, at position 3, the accelerated flow over the 5 m hedge is shown by a value of *VR* greater than 1.0. None of these effects is apparent at position 5. In general, therefore, it is likely that the incident flow on both the experimental building and the estate, is free from the local effects created by the hedges.

Analogue records of velocity were taken from the anemometers at 3 m, 5 m and 10 m on the fixed mast to the south-east of the experimental building during all recording periods, and analysed in the same way as the pressure records. The anemometers have a high frequency cut-off at about 0.5 Hz. An example of the power spectra from these three anemometers is shown in Fig.19.

Extreme values

Before applying digital filtering to the data, the number of data points in each record was 32,000. To check the reliability of maximum and minimum extremes, pressure values were also computed corresponding to certain percentiles of the probability distribution function. These were the 1 per cent (and 99 per cent) points corresponding to 320 values exceeded, and the 0.05 per cent (and 99.95 per cent) points corresponding to 16 values exceeded. These statistics will be less affected by false values, such as undetected "drop-outs" on the magnetic tapes, although precautions had been taken to eliminate these.

Figure 20 shows one of several consistent examples, comparing the pressure coefficients of 1/32-second duration on the walls of the experimental building for different percentile levels. The mean values are included for comparison, and as the probability distributions are not very skew these mean coefficients are virtually equivalent to the 50 per cent percentile. There is a smooth progression through the 1 per cent and 0.05 per cent percentile curves to the extreme value showing these extremes to be reliable. Similar results have been obtained for all averaging periods between 1/32 second and 32 seconds, and for other transducer positions on both the experimental building and on houses in the estate. For loading, extreme values are important, and these are often significantly higher than the 0.05 per cent percentiles; the extremes

have therefore been presented instead of percentiles, except for a few cases where the former were not calculated.

Tables 2 to 11 (pp.98–109) present these data for all the records discussed in this paper. The Tables also give values of the gust factor, g , defined by $g = (|\hat{p}| - |\bar{p}|)/\sigma_p$. The definition assumes, as is usual, that the mean and the peak values both have the same sign. Values of pressure coefficients are also tabulated for means taken over the record length, and for 2-second and 1/32-second durations.

Pressure coefficients

Throughout this paper, both for the experimental building and for the houses in the estate, pressure coefficients are based upon the velocity measurements made on the fixed mast near the experimental building. Since the anemometers do not respond to gusts of shorter duration than 2 seconds, both the 2-second and the 1/32-second pressure coefficients are based upon the 2-second velocity pressure, but mean pressure coefficients are based upon the mean velocity pressure averaged over the duration of the recording period (usually 1024 seconds).

Walls of the experimental building

Figure 21 compares the mean pressure coefficients on the windward wall of the experimental building when calculated in two different ways. Figure 22 makes the same comparison for the 1/32-second extreme values. The methods of calculation are:

- (i) To base the coefficients upon the appropriate duration velocity pressure at 10 m.
- (ii) To base the coefficients upon the appropriate duration velocity pressure at a height above ground level corresponding to the height of the pressure transducers.

The latter method is possibly better on the windward wall of a building especially if the building is tall. However, when the building is low-rise, when it is totally immersed in the roughness layer, and when coefficients are being calculated for positions on roofs, side walls and lee walls, the authors regard method (i) as the better way to present the experimental results. All the results in subsequent Figures are presented in this way. The method of basing coefficients upon the velocity pressure at the height of the top of the building is appropriate for design and is used in the present British Code of Practice [9]. For the presentation of experimental results and for the purpose of comparison with other full-scale low-rise research, it may, however, be useful to standardise coefficients by using the 10 m velocity pressure. This is particularly relevant for this project, where the ridge height of the experimental building varies between 5.7 m at 5° pitch and 8.8 m at 45° pitch. Figure 23 shows a typical pressure distribution on the walls of the experimental building with the wind blowing on to a minor face. This is the only record where the anemometers were in the wake of the experimental building. No allowance has been made for this.

Roof of experimental building

In Figs. 24(a), (b) and (c), distributions of mean pressure over the roof of the experimental building, in a skew wind, are compared for roof pitches of $22\frac{1}{2}^\circ$, 15° and 10° . The pressures are expressed as coefficients, $C_{\bar{p}}$, defined in the list of symbols. Figures 25(a), (b) and (c), show the same comparison for extreme pressures of 1/32-second duration in terms of the coefficient $C_{\hat{p}}$ (1/32 sec). In an area of building-induced turbulence such as this, it might have been expected that extreme-pressure coefficients would be greater in magnitude than mean-pressure coefficients, even when both are based upon q values for corresponding averaging periods. The coefficients $C_{\hat{p}}$ are, in fact, based on 2-second velocity pressures instead of 1/32-second; this will make $C_{\hat{p}}$ even greater. In general, however, for corresponding measurement positions, $C_{\hat{p}}$ (1/32 sec) $<$ $C_{\bar{p}}$. This result is an example of the problems of presenting and codifying this type of information. The pressure coefficients could be based upon gust velocities as in many Codes of Practice, or upon mean velocities for the duration of the record, which would be more in line with wind tunnel procedures. Further, the coefficients can be based on the velocity at 10 m or, alternatively, the velocity at the ridge height.

Table 12 (p.00) shows how the mean and peak pressure coefficients for transducer WR1C vary when calculated by these different methods. For each roof pitch, the largest differences in $C_{\hat{p}}$ are between those based on \bar{q} and \hat{q} . There are also smaller differences between those based on q_{10} and q_h . In particular, $C_{\hat{p}}$ values are of the order of -7.0 for the lower roof pitches when based on \bar{q}_h .

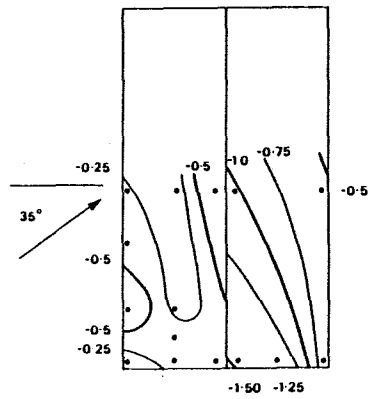
The estate

Figure 26 shows mean pressure coefficients on the houses through the middle of the estate for three different wind directions. Again these coefficients are based upon the velocity at 10 m taken from simultaneous measurements on the mast by the experimental building. These coefficients are rather erratic, as might be expected, owing to the effect of the buildings on each other.

Considering record A7 first, where the wind was blowing square-on to the terraces from the open country fetch, there is just one area of substantial pressure, on the windward wall of the windward house (76). All the other pressures are small, showing the large amount of shelter afforded by the first row of houses. On the other rows, there are small positive pressures on the windward walls and roofs, and small negative pressures on the leeward roof, but in two cases (58 and 33) the pressure on the lee wall is slight and positive. This occurs in alternate rows and may be due to eddy effects produced by the irregular spacing of the terraces, which are spaced in pairs as can be seen in Fig. 1

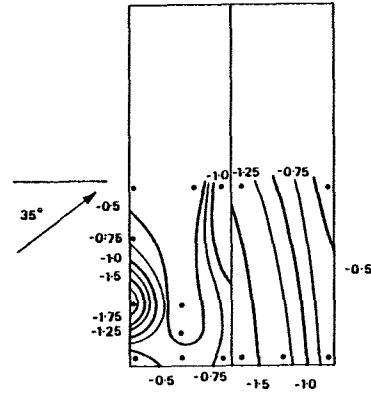
The same general pattern is repeated for record A5 where the wind is 40° from normal to the terraces. Again, there are significant positive coefficients on the windward wall of the windward terrace and again smaller erratic wall pressures further into the estate including the slight positive pressure on the lee wall of house 58. (Unfortunately, data from house 33 are not available for

(a) Record A11
Roof pitch 22.5°



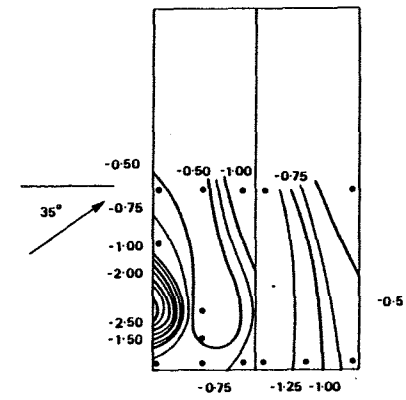
Mean C_p based on 10m mean velocity

(b) Record A12B
Roof pitch 15°



Mean C_p based on 10m mean velocity

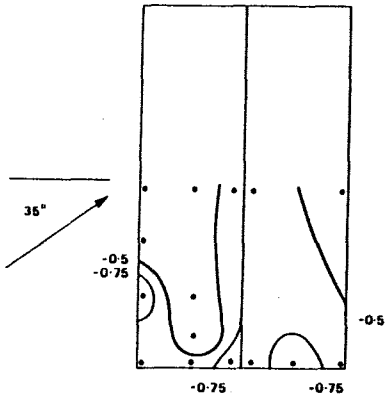
(c) Record A12A
Roof pitch 10°



Mean C_p based on 10m mean velocity

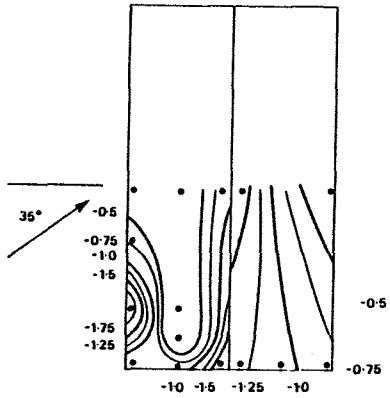
Fig.24. Mean pressure coefficients on roof of experimental building.

(a) Record A11
Roof pitch 22.5°



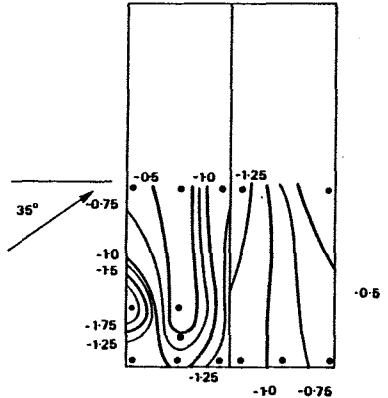
Extreme $\frac{1}{2}$ second C_p based on 10m extreme 2 second velocity

(b) Record A12B
Roof pitch 15°



Extreme $\frac{1}{2}$ second C_p based on 10m extreme 2 second velocity

(c) Record A12A
Roof pitch 10°



Extreme $\frac{1}{2}$ second C_p based on 10m extreme 2 second velocity

Fig.25. Peak pressure coefficients on roof of experimental building.

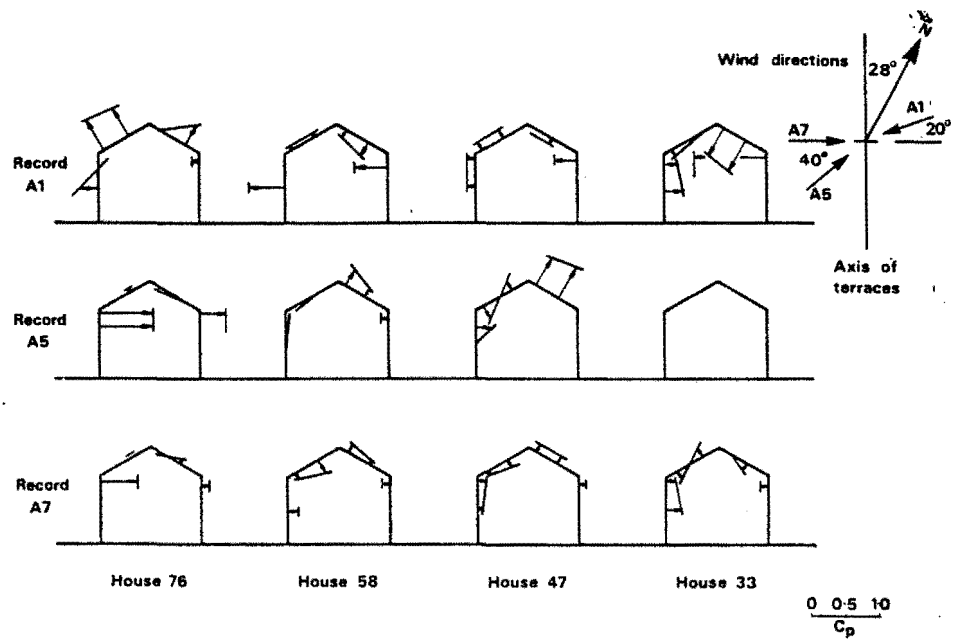


Fig.26. Mean pressure coefficients on houses in the estate for three different wind directions.

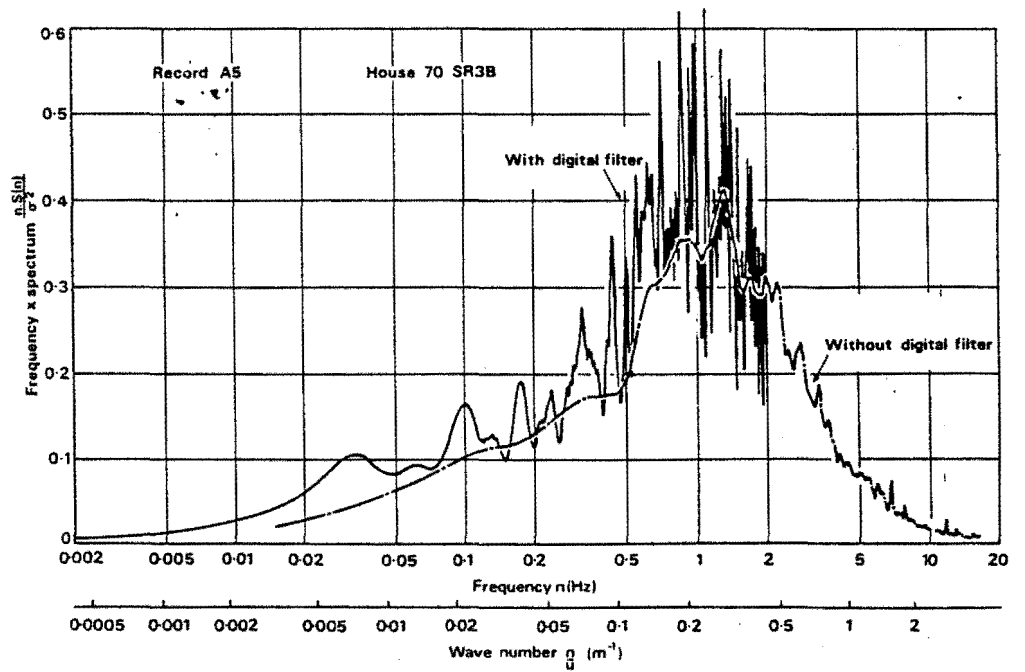


Fig.27. Comparison of a pressure spectrum computed over two different frequency bands.

this record to compare the pressure on that lee wall with record A7.) In this record, however, the suctions on the lee roofs are much greater than for the square-on wind (A7).

For record A1, in which the wind is blowing from the opposite direction, and where the upstream fetch is the urban terrain, the pressures are again confused. Although in the immediate wake of two uninstrumented terraces, the first house (33) shows the greatest positive pressures on the windward wall and roof, but also significant positive pressures on the lee wall. In fact, there is positive pressure over the whole house; this could indicate that the reference pressure was in error, but there was no evidence of this, and in any case the same reference pressure is used for all the houses. The next two houses show windward pressures and leeward suctions, although the values are quite small, while the last house (76) shows not only the largest suctions on the lee roof but also a large suction on the windward roof.

A full comparison of pressures in the estate with those on the isolated experimental building is not presented here. However, a comparison of roof suctions may be made between record A5 in Fig.26, and record A11 in Fig.24(a), the roof pitch being identical and the wind direction the same to within 5° . For an east-west section through the centre of the experimental building it will be seen that the suctions are very much greater than those on the roofs of the estate. Moreover, the whole roof is experiencing suction, whereas in the estate, for this wind direction, no roof is entirely subjected to suction.

These few results show the erratic nature of the pressure distribution over groups of houses and the marked difference between this case and that of an isolated building in the same incident wind conditions.

Power spectra

Figure 27 shows the power spectrum of pressure fluctuations for a measurement point on the roof of house 70 in a skew wind, calculated over two different bandwidths. Here the spectrum contains high frequency components extending beyond 2 Hz, which is the Nyquist frequency for the data after application of the digital filter. The two curves show the spectrum calculated with the digital filter and also directly from the raw digitised data without the filter. In the latter case, the Nyquist frequency is 16 Hz. In most cases, the power spectra do not extend beyond 2 Hz and, except in Fig.28, the digital filter has been used.

Figure 28 shows power spectra of three signals; these are the free wind speed at 10 m, the pressure recorded on the windward gable end of house 70, and the pressure recorded on the roof of the same house near the ridge. It will be seen that the main peaks of both pressure spectra are shifted towards higher frequencies compared with the velocity spectrum, and that, in the case of the roof pressures close to the ridge, the frequency shift is greater. This comparison clearly demonstrates the introduction of small-scale turbulence by the building itself.

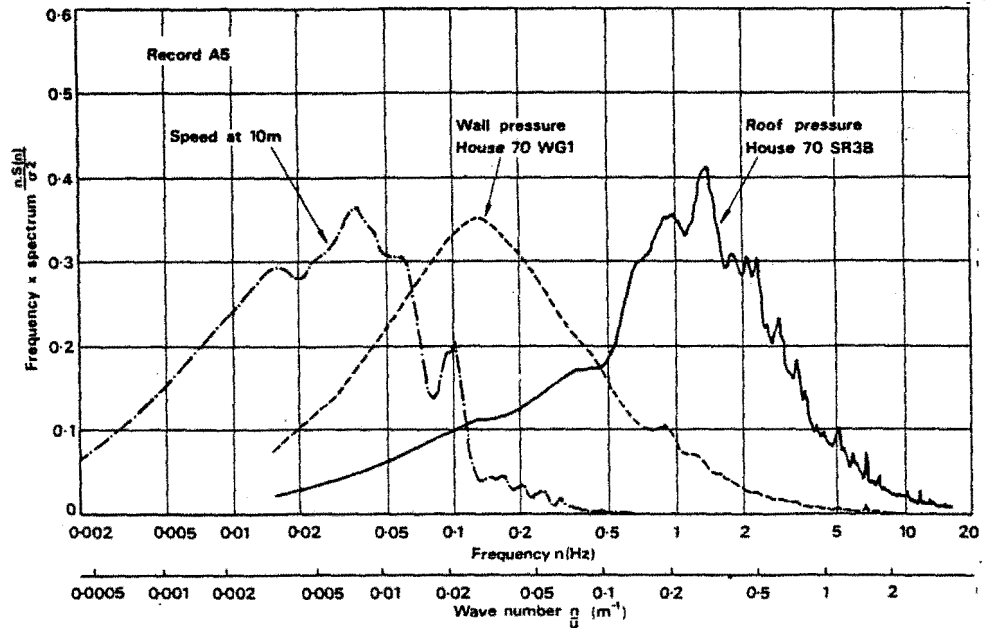


Fig.28. Comparison of velocity spectrum with wall and roof pressure spectra.

In Fig.29, eight pressure spectra are shown for different positions on the walls and roof of the experimental building for a wind blowing normal to the major face. The spectra are of three distinct types. The first is shown in Fig.29(a), which is for a pressure signal from the windward wall (3WW3). This spectrum has one principal peak and is very similar to the 3 m velocity spectrum shown in Fig.19. The similarity is to be expected since this pressure transducer is sited where there is little building-induced turbulence and the free stream velocity is almost completely recovered as a pressure. The second type is shown by the pressure signals on the windward roof (Figs.29(b) and (c)). These spectra are characterised by the absence of the main peak of the velocity spectrum, the spectrum being shifted upwards in frequency, especially in the case of WR3A. The mean and rms pressures for this position are very low. The shape of the spectrum is explained if it is assumed that the flow is re-attached in this region of low pressure, and the free-stream velocity fluctuations are not recovered as pressures. Lower down the roof (WR1D) the mean pressure is larger, but the same general shape of spectrum suggests, principally, building-induced turbulence. The other five spectra (Figs.29(d)–(h)) belong to the third type. They are for pressures measured on the leeward wall and roof, the side walls, and the internal pressure. These spectra all show two principal peaks; the lower frequency peak corresponds to the peak in the free-stream velocity spectrum and the higher frequency peak corresponds to the superimposed building-induced turbulence. The internal pressure is largely governed by the leakage of air through the gable ends which were the most permeable

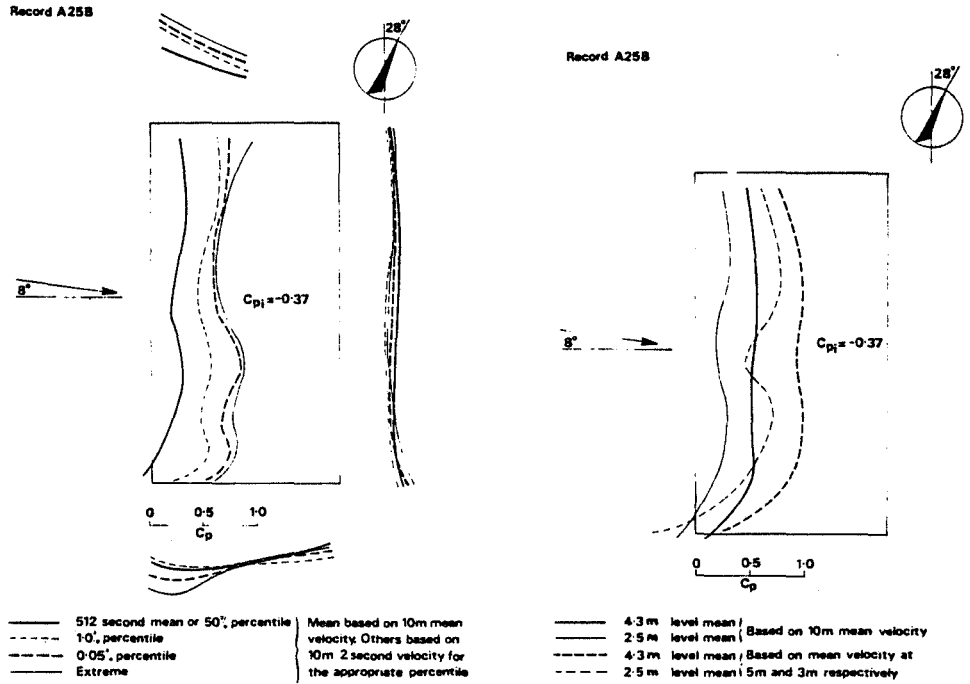


Fig. 20. Plan of experimental building showing wall pressure coefficients at 2.5 m level; 1/32-second duration.

Fig. 21. Mean wall pressure coefficients; comparison of two methods of calculation.

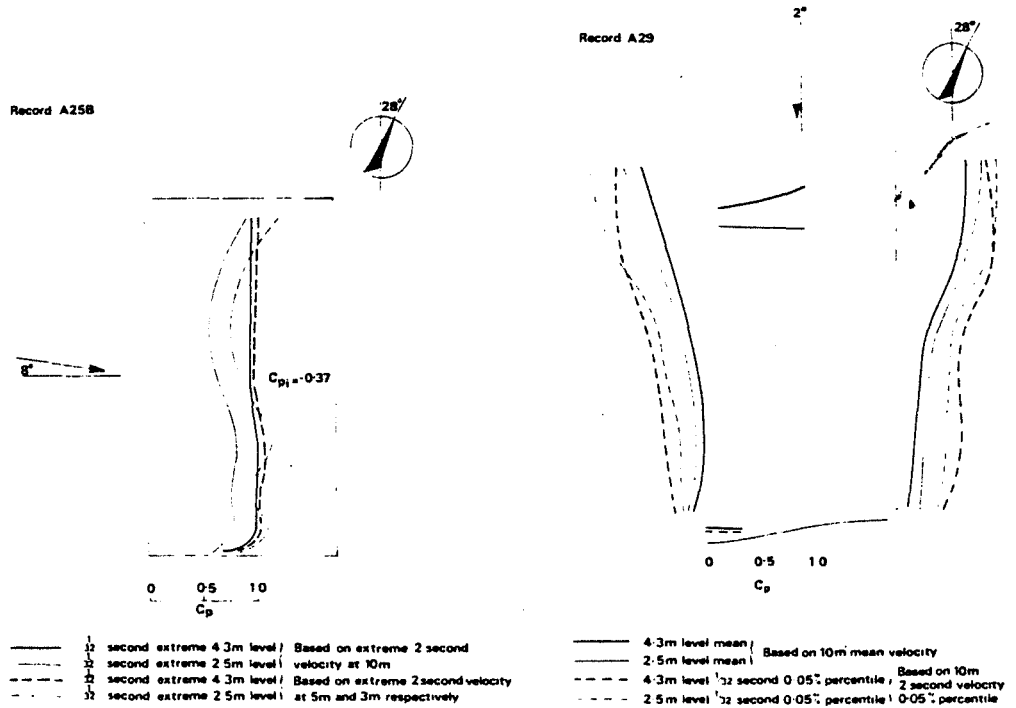


Fig. 22. Peak wall pressure coefficients; comparison of two methods of calculation.

Fig. 23. Mean and peak wall pressure coefficients for wind normal to gable end.

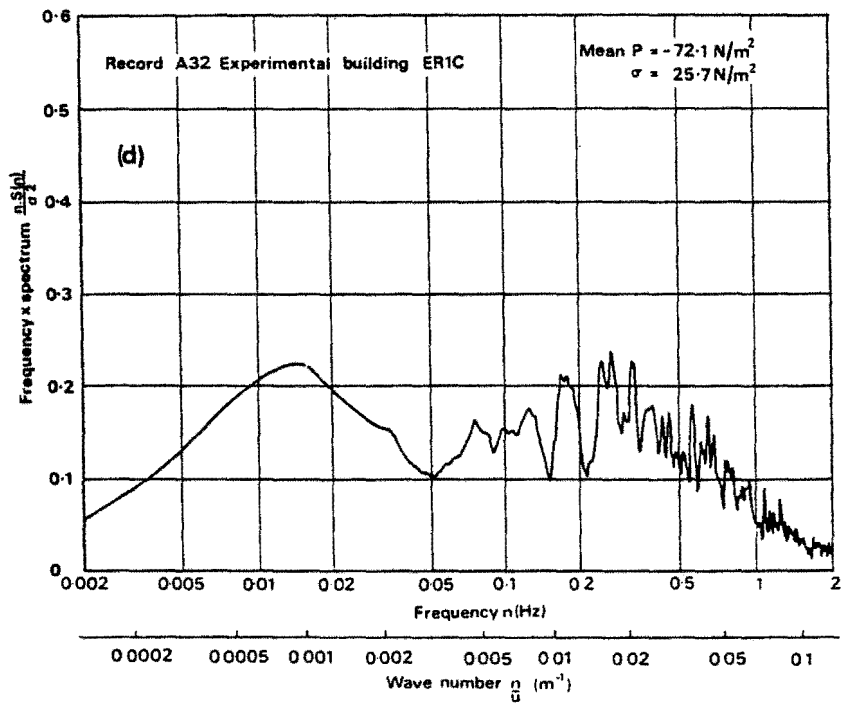
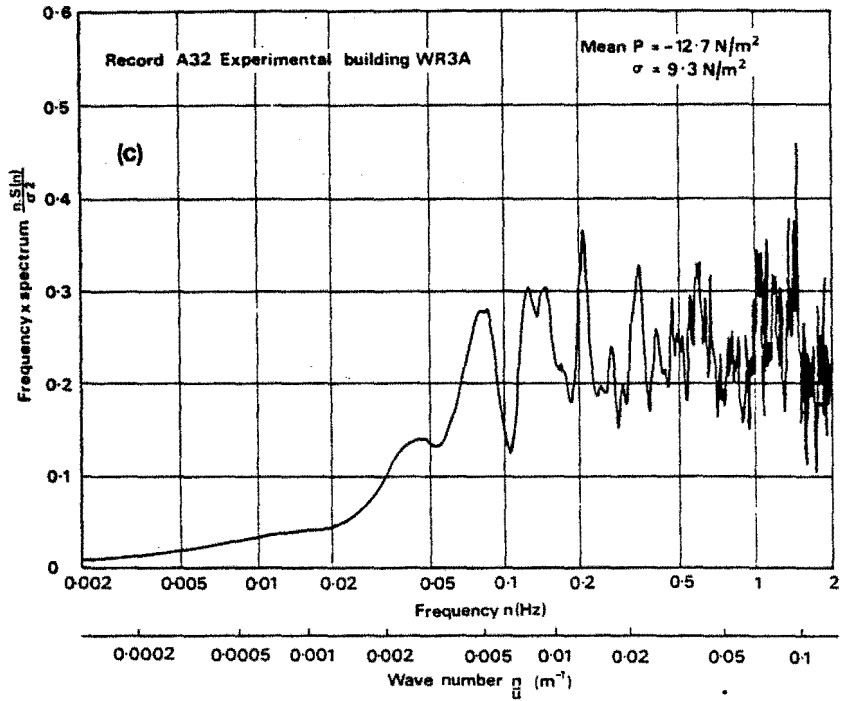


Fig.29. (continued)

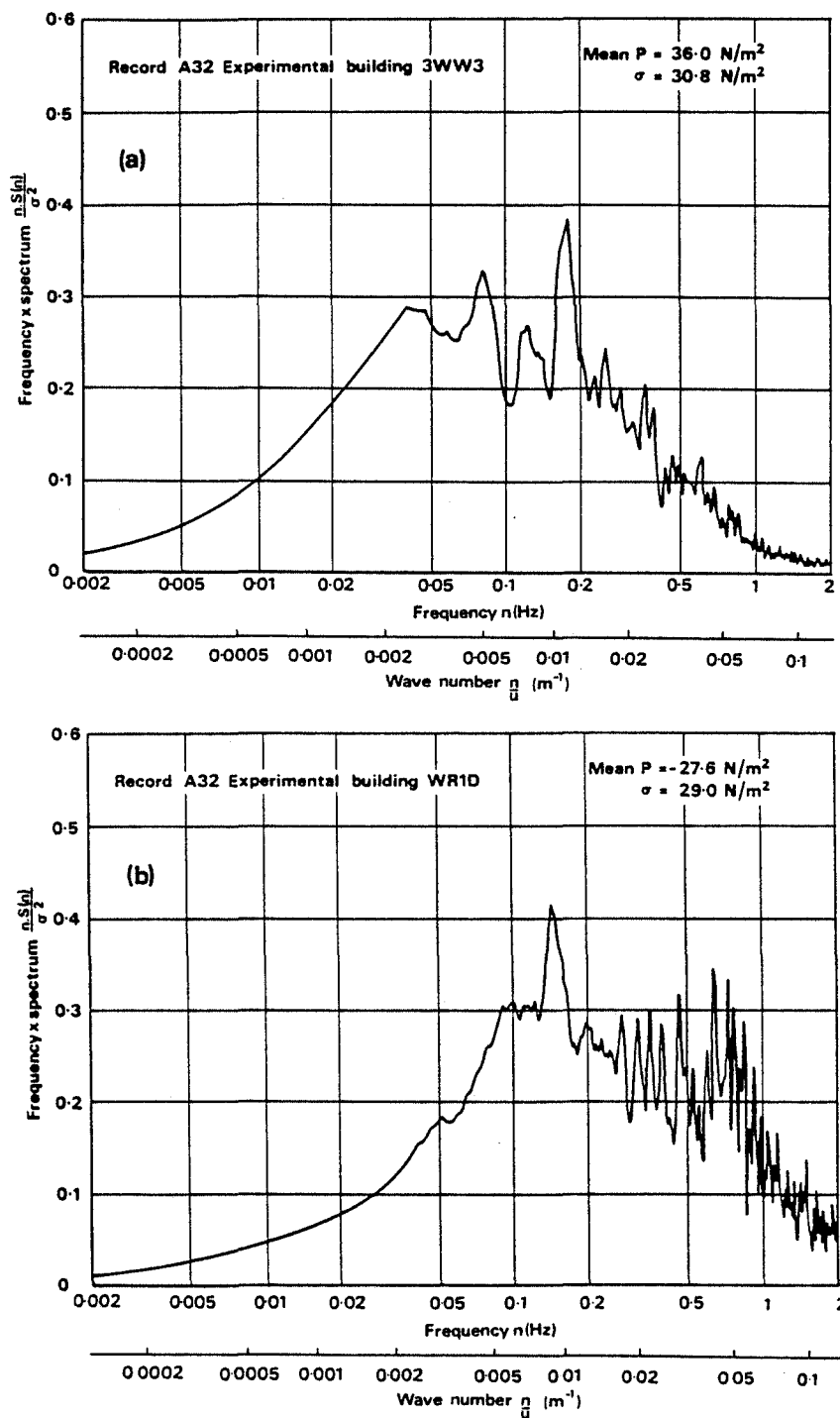


Fig.29. Examples of pressure spectra at various positions on the experimental building.

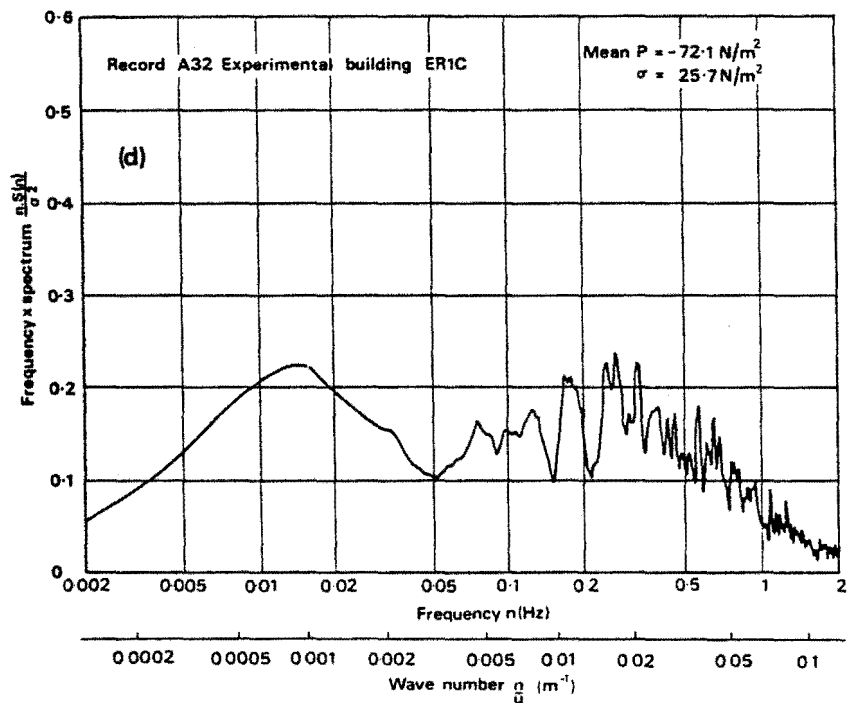
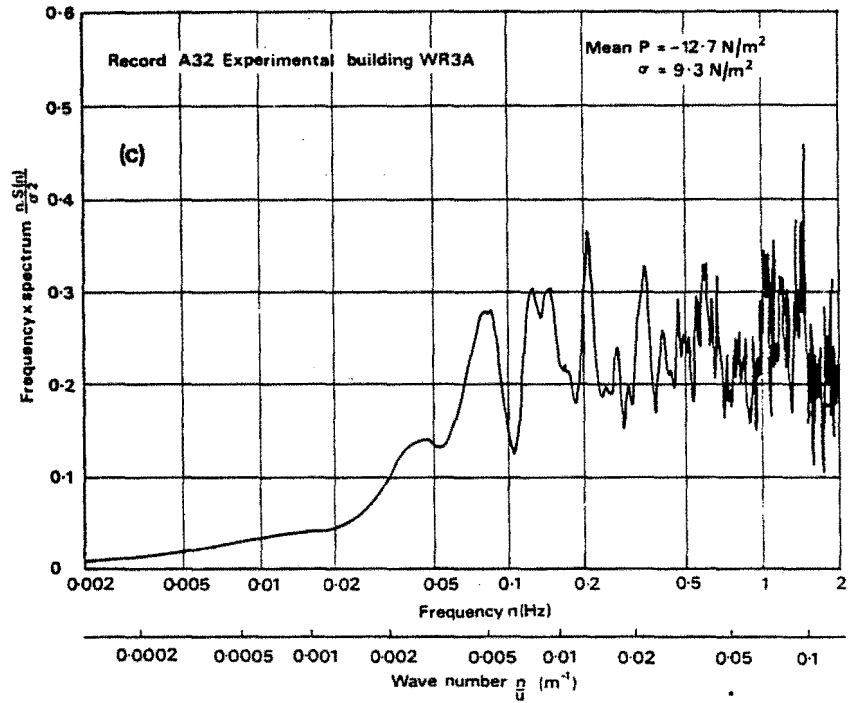


Fig.29. (continued)

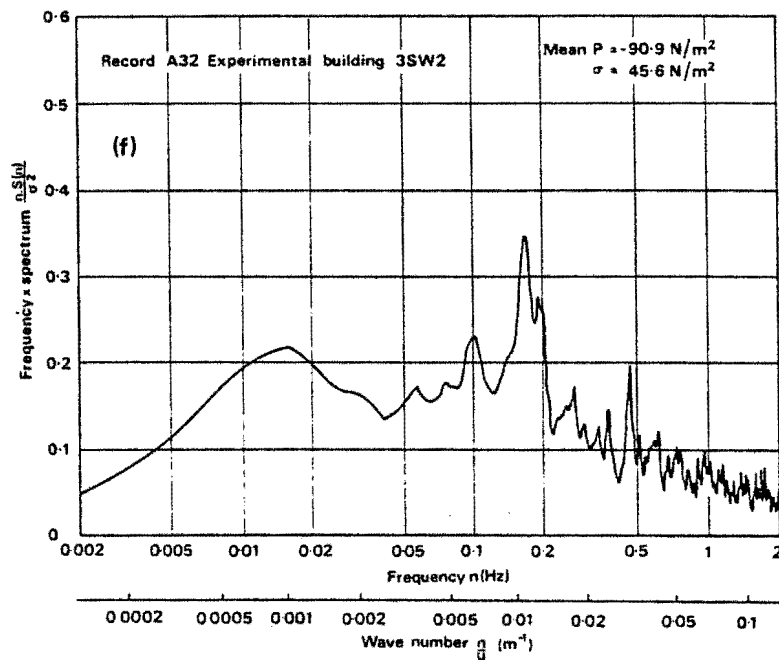
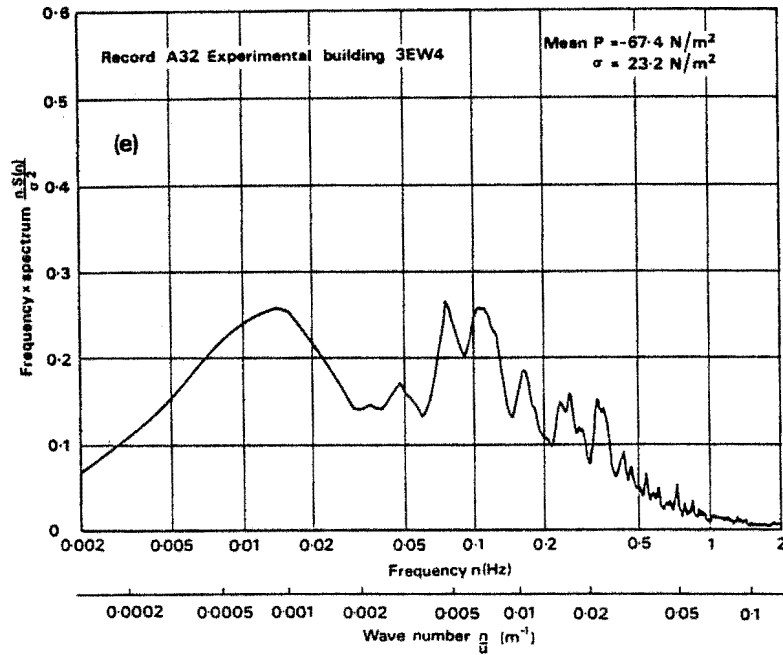


Fig.29. (continued)

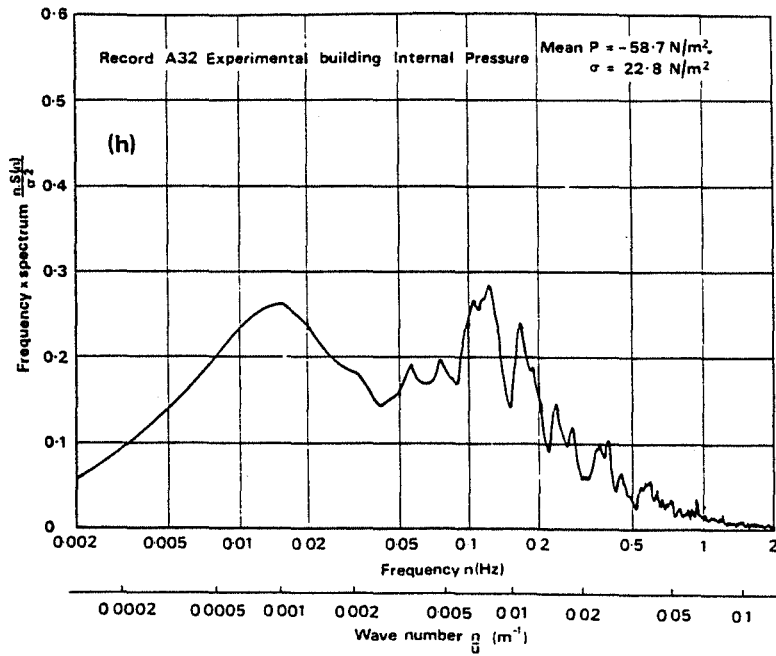
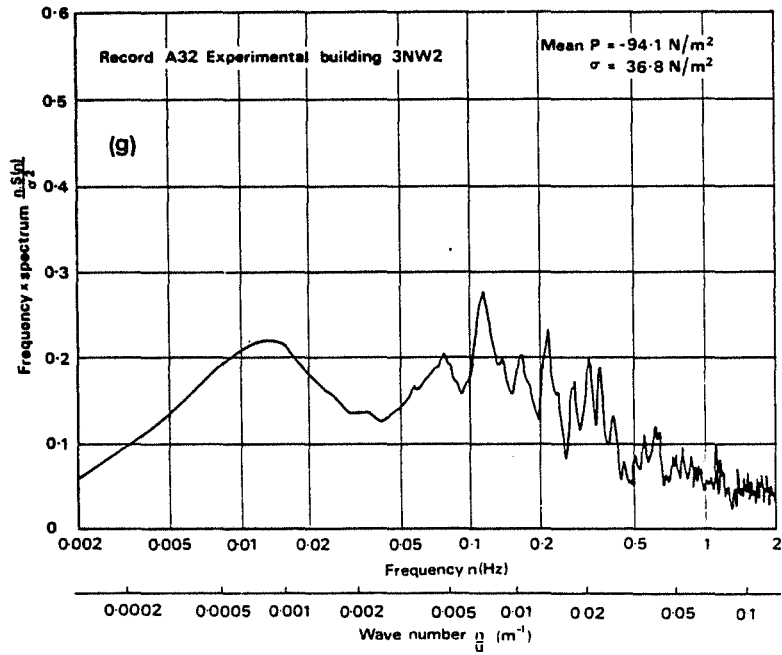


Fig.29. (continued)

parts of the building. The similarity of shape between the spectra for the end walls and for the internal pressure, demonstrates the rapidity with which fluctuations of pressure were transferred to the interior of the building. Measurements have also been made of loft pressures in house 76, which is typical of modern construction in the United Kingdom, and results of this aspect of the experiments will be published elsewhere.

8. Concluding remarks

This paper presents and discusses some of the initial results of pressure measurements on a group of low-rise buildings. Considerable problems were encountered in setting-up this project; these were not previously encountered in measurements on tall buildings, and consequently, instrumentation and analysis techniques have been modified.

Some of the results have been largely predictable, others have been somewhat surprising. Being probably the first major full-scale investigation on low-rise buildings, all these results are particularly useful and should eventually provide designers with valuable information which they can use with confidence. This paper presents initial results and clarifies some points about wind pressures on low-rise buildings, but there are further points that still need clarification.

The measurements at Aylesbury have now been concluded: numerous records have yet to be analysed and of those already analysed not all have been discussed in this paper. In addition, only a limited range of results have been mentioned and further aspects will be covered in the near future. These include the effects of permeability on internal pressures, the variations of overall structural loads as roof pitch is varied, the effects of a large eaves overhang on pressures and loads, the variation of peak gust factors, a discussion on cross-correlations between pairs of signals, and velocity measurements in between buildings in urban areas.

Acknowledgements

The authors wish to thank Aylesbury Borough Council and their tenants for their co-operation at all stages of this experiment. They also gratefully acknowledge the assistance provided by the Environmental Sciences Research Unit at Cranfield and all the staff of the Wind Loading Section at the Building Research Station. The work described has been carried out as part of the research programme of the Building Research Establishment of the Department of the Environment, and this paper is published by permission of the Director.

Nomenclature

\bar{u}_{10}	mean velocity at 10 m over record length
\hat{u}_{10}	peak 2-second velocity during record
$\bar{\beta}$	mean wind direction relative to true north
$\bar{\theta}$	mean wind direction relative to the axis of the estate and experimental building
\bar{p}	mean pressure over record length
p_{\max}, p_{\min}	extreme 1/32-second values except for Tables 9, 10 and 11 where they are 0.05 per cent percentiles
\hat{p}	denotes p_{\max} or p_{\min} as appropriate
σ_p	rms pressure calculated over record length
g	$(\hat{p} - \bar{p})/\sigma_p$
$C_{\bar{p}}$	\bar{p}/\bar{q}_{10}
$C_{\hat{p}}(2 \text{ sec})$	$\hat{p}(2 \text{ sec})/\hat{q}_{10}(2 \text{ sec})$
$C_{\hat{p}}(1/32 \text{ sec})$	$\hat{p}(1/32 \text{ sec})/\hat{q}_{10}(2 \text{ sec})$
C_{pi}	internal pressure coefficient based on 10 m mean velocity
q	dynamic pressure = $\frac{1}{2}\rho u^2$ where ρ is density of air
\bar{q}	$\frac{1}{2}\rho \bar{u}^2$
\hat{q}	$\frac{1}{2}\rho \hat{u}^2$
q_{10}	$\frac{1}{2}\rho u_{10}^2$
q_h	$\frac{1}{2}\rho u_h^2$

References

- 1 C.W. Newberry, K.J. Eaton and J.R. Mayne, The nature of gust loading on tall buildings, Proc. Int. Seminar on Wind Effects on Buildings and Structures, Ottawa, September 1967. (Also BRS Current Paper CP 66/68.)
- 2 C.W. Newberry, K.J. Eaton and J.R. Mayne, Wind loading of a tall building in an urban environment, Proc. Symp. on Buildings and Structures, University of Technology, Loughborough, April 1968. (Also BRS Current Paper CP 59/68.)
- 3 C.W. Newberry, K.J. Eaton and J.R. Mayne, Wind loading on tall buildings — further results from Royex House, Ind. Aerodynamics Abstr., 4 (4) (1973). (Also BRE Current Paper CP 29/73.)
- 4 C.W. Newberry, K.J. Eaton and J.R. Mayne, Wind pressures on the Post Office Tower, London, Proc. Int. Conf. on Wind Effects on Buildings and Structures, Tokyo, September 1971. (Also BRS Current Paper CP 37/71.)
- 5 C.W. Newberry, K.J. Eaton and J.R. Mayne, Wind pressure and strain measurements at the Post Office Tower, BRE Current Paper CP 30/73, November 1973.
- 6 K.J. Eaton and J.R. Mayne, Instrumentation and analysis of full-scale wind pressure measurements, Proc. Symp. on Instrumentation and Data Processing for Industrial Aerodynamics, Nat. Phys. Lab., Teddington, November 1968. (Also BRS Current Paper CP 1/69.)
- 7 C.W. Newberry, K.J. Eaton and J.R. Mayne, Wind loading on Vickers Tower, Millbank, Building, 219 (1970) 53–56. (Also BRS Current Paper CP 35/70.)
- 8 J.B. Menzies, Wind damage to buildings in the United Kingdom 1962–1969, Building, 221 (1971) 67–76. (Also BRS Current Paper CP 35/71.)
- 9 British Standard Code of Practice CP3, Chap. V, Part 2, 1972, Wind loads, British Standards Institution, London.
- 10 J.R. Mayne, A wind-pressure transducer, J. Phys. E, 3 (1970) 248–250. (Also BRS Current Paper CP 17/70.)

Table 2 Record A1

	76 WW2	76 WW2	76 WR1	76 WR2	76 ER2	76 ER1	76 EW1	58 WW1	58 WW2	58 WR1	58 WR2	58 ER2	58 ER1	58 EW1	47 WW1	47 WW2	47 WR1	47 WR2	47 ER2	47 ER1	47 EW1	33 WW2
\bar{p} (N/m ²)	-11	3	-18	-16	1	-9	4	-18	-2	-2	-2	4	7	17	-3	-3	-3	-5	2	3	11	10
σ_p (N/m ²)	10	10	11	15	10	13	17	8	1	8	9	8	9	20	3	3	3	5	5	8	15	6
P_{max} (N/m ²)	20	36	33	28	54	71	113	68	5	22	33	45	59	165	15	16	18	30	55	70	132	40
P_{min} (N/m ²)	-76	-64	-77	-128	-68	-66	-73	-59	-10	-64	-30	-34	-37	-43	-18	-28	-55	-53	-28	-24	-98	-18
g	6.3	5.9	5.4	7.7	7.0	4.8	6.6	5.8	5.7	7.6	8.8	5.5	5.7	7.5	5.3	7.6	16.9	9.0	9.9	8.0	8.1	4.7
$C_{\bar{p}}$	-0.31	0.09	-0.53	-0.47	0.03	-0.26	0.12	-0.53	-0.06	-0.06	-0.06	0.12	0.21	0.50	-0.09	-0.09	-0.09	-0.15	0.06	0.09	0.32	0.29
$C_{\bar{p}}$ (2 sec)	-0.40	-0.27	-0.34	-0.55	-0.22	0.22	0.48	0.03	-0.04	-0.25	-0.31	0.22	0.30	0.79	-0.07	-0.09	-0.15	-0.21	0.17	0.34	0.41	0.25
$C_{\bar{p}}$ (1/32 sec)	-0.55	-0.46	-0.56	-0.92	-0.49	0.52	0.82	0.49	-0.07	-0.47	-0.58	0.33	0.43	1.2	-0.13	-0.20	-0.40	-0.38	0.40	0.50	0.95	0.29

	33 WW2	33 WR1	33 WR2	33 ER2	33 ER1	33 EW1	70 WG1	70 NR1	70 NR2A	70 NR2B	70 SR1A	70 SR1B	70 SR2A	70 SR2B	70 SR3A	70 SR3B	83 SG1A	83 SG2	83 SG1B	82 NG1B	82 NC2	82 NC1A
\bar{p} (N/m ²)	7	4	1	14	18	36	-2	-2	-6	-9	-4	-3	-2	1	-3	-6	-16	-23	-26	-14	-28	-57
σ_p (N/m ²)	7	8	11	8	11	23	6	7	1	7	5	7	6	7	5	10	9	14	24	12	23	32
P_{max} (N/m ²)	40	41	48	58	86	154	23	40	0	16	21	34	30	42	27	14	19	23	74	38	51	49
P_{min} (N/m ²)	-26	-51	-56	-14	-18	-37	-36	-41	-10	-87	-32	-72	-16	-54	-42	-185	-77	-144	-215	-109	-184	-247
g	4.5	5.5	4.9	5.7	6.2	5.1	5.7	5.2	2.9	11.3	5.6	10.5	7.9	7.0	7.3	18.4	6.7	8.8	7.8	7.7	7.0	6.0
$C_{\bar{p}}$	0.21	0.12	0.03	0.41	0.53	-	-0.06	-0.06	-0.18	-0.26	-0.12	-0.09	-0.06	0.03	-0.09	-0.18	-0.47	-0.68	-0.76	-0.41	-0.76	-1.67
$C_{\bar{p}}$ (2 sec)	0.24	-0.19	-0.24	0.32	0.46	0.83	-0.16	-0.17	-0.06	-0.29	-0.14	-0.28	-0.13	-0.10	-0.12	-0.32	-0.37	-0.63	-0.87	-0.39	-0.84	-1.16
$C_{\bar{p}}$ (1/32 sec)	0.29	-0.37	-0.40	0.42	0.62	1.12	-0.26	-0.30	-0.07	-0.63	-0.23	-0.53	-0.34	-0.39	-0.31	-1.34	-0.55	-1.04	-1.56	-0.79	-1.34	-1.79

Duration 1024 seconds; $\bar{u}_{10} = 7.6$ m/s; $\hat{u}_{10} = 15.0$ m/s; $\bar{\beta} = 40^\circ$; $\hat{\beta} = 70^\circ$.

Table 1 Details of records taken at Aylesbury

Record no	Date	Time GMT	$\bar{\beta}$	$\bar{\theta}$	\bar{u}_{10} (m/s)	\hat{u}_{10} (m/s)	Roof pitch of experimental building
A1	12. 3.72	13. 59	40°	70°	7.6	15.0	*
A5	25. 5.72	23.24	200°	230°	6.1	13.2	22.5°
A7	26. 5.72	12. 43	235°	265°	11.9	18.6	22.5°
A11	1.12.72	12.06	205°	235°	9.4	20.9	22.5°
A12A	1.12.72	13.38	205°	235°	8.4	15.6	10.0°
A12B	1.12.72	14.07	205°	235°	8.4	14.7	15.0°
A25B	12.11.73	15.48	250°	280°	8.4	12.9	22.5°
A29	14.12.73	16.04	330°	0°	8.6	13.2	22.5°
A31B	8. 1.74	14.35	150°	180°	13.3	21.2	22.5°
A32	8. 1.74	15.55	235°	265°	14.3	24.4	22.5°

$\bar{\beta}$ Mean wind direction relative to true north.

$\bar{\theta}$ Mean wind direction relative to N-S axis of experimental building.

\bar{u}_{10} Mean wind speed averaged over the length of the record.

\hat{u}_{10} Maximum 2 second speed during record.

* Results refer to houses in estate.

Table 3 Record A5

	WR1A	WR1E	WR3A	WR3B	WR3C	WR3E	WR4A	WR4E	ER1A	ER1B	ER2A	ER3A	3WW3	3WW4	3WW5	3WW6	3WW7	5WW3	5WW7	5EW1	5EW3	5EW1	5SW1
\bar{p} (N/m ²)	7	-13	12	9	6	4	1	0	20	-22	-17	-5	7	7	11	11	8	-9	17	-28	-24	-24	-14
σ_p (N/m ²)	6	8	15	9	5	6	1	1	9	9	13	2	12	12	15	14	13	15	17	11	9	10	17
p_{max} (N/m ²)	40	37	64	47	29	37	33	16	65	6	14	6	63	66	87	87	89	55	105	-2	-1	-1	52
p_{min} (N/m ²)	-38	-57	-124	-24	-7	-16	-4	-8	-3	-75	-92	-19	-31	-37	-38	-42	-76	-49	-79	-84	-67	-75	-116
g	7.5	6.25	9.05	4.22	4.6	5.5	32	16	5	5.9	5.8	7	4.7	4.9	5.1	6.1	6.2	4.3	5.7	5.1	4.8	5.1	6
$C_{\bar{p}}$	0.31	-0.58	0.53	0.40	0.27	0.18	0.04	0	0.89	-0.97	-0.75	-0.22	0.31	0.31	0.49	0.49	0.35	-0.40	0.75	-1.24	-1.06	-1.06	-0.62
$C_{\hat{p}}$ (2 sec)	0.14	-0.35	-0.68	0.35	0.21	0.26	0.01	0.01	0.51	-0.49	-0.69	-0.10	0.46	0.48	0.59	0.55	0.53	0.39	0.69	-0.66	-0.57	-0.59	-0.60
$C_{\hat{p}}$ (1/32 sec)	0.38	-0.54	-1.17	0.44	0.28	0.35	0.31	0.15	0.61	-0.71	-0.87	-0.18	0.60	0.62	0.82	0.92	0.84	0.52	0.99	-0.79	-0.64	-0.71	-1.09

	5SW2	5SW3	5SW4	3NW1	3NW2	76WR2	76WR2	76ER2	76ER1	76EW1	58WW1	58WW2	58WR1	58WR2	58ER2	58ER1	58EW1	47WW1	47WW2	47WR1	47WR2	47ER2	47ER1	47EW1
\bar{p} (N/m ²)	-16	-13	-11	-17	-21	16	-1	1	1	-9	0	1	1	0	-6	-2	2	0	8	6	-2	-11	-12	-5
σ_p (N/m ²)	18	9	7	6	11	11	5	5	5	4	8	1	7	6	11	5	5	7	8	6	4	5	5	5
p_{max} (N/m ²)	44	31	21	-1	-1	117	27	49	18	4	36	7	31	28	24	17	23	42	72	54	37	4	8	13
p_{min} (N/m ²)	-111	-64	-54	-79	-74	-26	-23	-13	-46	-33	-57	-10	-35	-24	-69	-60	-30	-43	-28	-33	-21	-68	-55	-33
g	5.3	5.7	6.1	7.7	4.8	9.2	5.5	10.1	8.3	5.5	7.0	6.4	5	5.1	5.7	12.1	5.4	6.4	7.7	7.7	9.7	10.4	7.9	6
$C_{\bar{p}}$	-0.71	-0.58	-0.49	-0.75	-0.93	0.79	-0.04	0.04	0.04	-0.4	0	0.04	0.04	0	-0.27	-0.09	0.09	0	0.35	0.27	-0.09	-0.49	-0.53	-0.22
$C_{\hat{p}}$ (2 sec)	-0.64	-0.39	-0.41	-0.45	-0.55	0.60	0.12	0.19	-0.21	-0.26	-0.21	-0.03	-0.18	0.12	-0.39	-0.12	-0.11	-0.12	0.44	0.25	0.10	-0.34	-0.33	-0.24
$C_{\hat{p}}$ (1/32 sec)	-1.05	-0.60	-0.51	-0.75	-0.70	1.1	0.25	0.48	-0.43	-0.31	-0.54	-0.09	-0.33	0.27	-0.65	-0.58	-0.28	-0.41	0.68	0.51	0.35	-0.64	-0.52	-0.31

Duration 1024 seconds; \bar{u}_{10} 6.1 m/s; \bar{u}_5 5.8 m/s; \bar{u}_3 6.8 m/s; \bar{u}_{10} 13.2 m/s; \hat{u}_5 11.3 m/s; \hat{u}_3 10.5 m/s; $\bar{\beta}$ 200°, $\bar{\theta}$ 230°.

Table 5 Record A11

	WR1A	WR1C	WR1D	WR1E	WR3A	WR3B	WR3C	WR3E	WR4A	WR4E	SSW1	SSW2	SSW4
\bar{p} (N/m ²)	-9	-44	-17	-14	-14	-15	-11	-11	-26	-39	-13	-11	-17
σ_p (N/m ²)	12	33	11	6	13	8	5	4	19	20	25	27	9
p_{max} (N/m ²)	85	103	38	18	39	23	7	10	34	12	83	75	18
p_{min} (N/m ²)	-82	-255	-86	-51	-159	-55	-41	-38	-211	-169	-138	-161	-76
g	7.8	6.4	6.3	6.2	11.1	5	6	6.8	9.7	6.5	5	5.6	6.6
C_p	-0.17	-0.81	-0.31	-0.26	-0.26	-0.28	-0.20	-0.20	-0.48	-0.72	-0.24	-0.20	-0.31
C_p (2 sec)	0.19	-0.62	-0.20	-0.15	-0.33	-0.18	-0.14	-0.13	-0.61	-0.55	-0.32	-0.39	-0.22
C_p (1/32 sec)	-0.31	-0.95	-0.32	-0.19	-0.60	-0.21	-0.15	-0.14	-0.79	-0.63	-0.51	-0.60	-0.28

	ER1A	ER1B	ER2A	ER2A	ER3B	SWW3	SWW4	SWW5	SWW6	SWW7	SWW3	SWW7
\bar{p} (N/m ²)	-39	-34	-70	-81	-55	13	16	23	24	17	20	32
σ_p (N/m ²)	16	13	31	36	26	16	18	23	23	17	17	28
p_{max} (N/m ²)	-4	58	-22	41	-16	98	117	167	167	80	143	214
p_{min} (N/m ²)	-146	-108	-251	-196	-180	-33	-31	-38	-60	-147	-31	-130
g	6.7	7.1	5.8	3.4	4.8	5.3	5.5	6.3	6.2	7.6	7.2	6.5
C_p	-0.72	-0.63	-1.29	-1.49	-1.01	0.24	0.29	0.42	0.44	0.31	0.37	0.59
C_p (2 sec)	-0.43	-0.34	-0.89	-0.68	-0.87	0.28	0.34	0.47	0.42	-0.19	0.35	0.56
C_p (1/32 sec)	-0.54	-0.40	-0.94	-0.73	-0.87	0.37	0.44	0.63	0.62	-0.55	0.53	0.80

Duration 1024 seconds; $\bar{u}_{10} = 9.4$ m/s; $\bar{u}_3 = 8.3$ m/s; $\hat{u}_{10} = 20.9$ m/s; $\hat{u}_3 = 14.8$ m/s; $\bar{\beta} = 205^\circ$; $\bar{\theta} = 235^\circ$.

Table 4 Record A7

	76WW2	76WR2	76ER2	76ER1	76EW1	56WW1	56WR2	56WR1	56WR2	56ER2	56ER1	56EW1	47WW1	47WR2	47WR1	47WR2	47ER2	47ER1	47EW1	33WW1	33WR2	33WR1	33WR2	33ER2
\bar{p} (N/m ²)	47	-5	2	-6	-11	13	-1	9	16	-5	0	8	8	13	7	6	-10	-11	-9	21	18	21	-6	-3
σ_p (N/m ²)	22	9	14	15	12	15	3	15	15	14	11	9	12	15	12	8	10	10	7	15	17	17	12	22
P max (N/m ²)	192	52	115	35	28	140	20	120	104	44	64	53	116	111	76	67	20	23	13	100	133	161	72	50
P min (N/m ²)	-36	-54	-41	-157	-69	-53	-13	-49	-43	-116	-115	-34	-56	-61	-75	-21	-79	-72	-53	-66	-118	-57	-48	-166
g	6.5	5.2	7.0	10.2	4.9	8.8	7.4	7.3	6.0	7.8	10.0	5.0	9.3	6.4	5.6	7.8	7.2	6.3	5.9	5.2	6.7	6.3	5.5	7.6
C \bar{p}	0.54	-0.06	-0.02	-0.07	-0.13	0.15	-0.01	0.10	0.19	-0.14	0	0.09	0.09	0.15	0.08	0.07	-0.12	-0.13	-0.10	0.24	0.21	0.24	0.07	-0.03
C \hat{p} (2 sec)	0.64	-0.12	0.29	-0.27	-0.21	0.34	0.05	0.31	0.31	-0.29	-0.20	0.15	0.30	0.32	0.19	0.15	-0.17	-0.18	-0.19	0.35	0.42	0.42	0.15	-0.54
C \hat{p} (1/32 sec)	0.90	-0.26	0.54	-0.74	-0.33	0.66	0.09	0.56	0.49	-0.55	-0.54	0.25	0.55	0.52	0.36	0.31	-0.37	-0.34	-0.25	0.47	0.62	0.76	0.34	-0.78

	33ER1	33EW1	70WG1	70NR1	70ER1A	70SR1B	70ER1A	70SR2B	70SR3A	70SR3B	83SC1A	83SG2	83SC1B	82NG1B	82NG2	82NG1A	WR1A	WR1E	WR3A	WR3B	WR3C	WR3E	WR4A	WR4E
\bar{p} (N/m ²)	11	10	69	-20	-43	-20	-31	37	-47	6	-51	-27	-11	6	-3	-4	-11	-16	18	24	21	40	1	0
σ_p (N/m ²)	18	9	31	23	25	14	24	13	36	6	22	16	10	32	15	11	18	29	23	20	16	21	1	1
P max (N/m ²)	75	45	264	106	30	43	67	115	49	42	25	30	25	148	157	58	47	145	130	117	92	156	6	4
P min (N/m ²)	-148	95	-42	-238	-222	-126	-172	-71	-254	-197	-240	-177	-69	-171	-90	-59	-112	-190	-66	-43	-32	-27	-4	-4
g	7.8	9.7	6.2	9.4	7.3	7.3	5.9	6.1	5.7	34.4	8.6	5.2	5.7	5.2	10.1	5.1	5.6	9.2	4.9	4.2	4.4	5.5	5.0	4.0
C \bar{p}	0.13	-0.12	0.80	-0.23	-0.50	-0.23	-0.36	0.43	-0.54	0.07	-0.59	-0.31	-0.13	0.07	-0.03	-0.05	-0.13	-0.19	0.21	0.28	0.24	0.46	0.01	0
C \hat{p} (2 sec)	-0.41	-0.07	0.77	-0.34	-0.60	-0.31	-0.61	0.30	-0.61	-0.04	-0.62	-0.46	-0.18	-0.46	0.25	-0.16	-0.29	-0.44	0.40	0.39	0.34	0.55	0.02	0.01
C \hat{p} (1/32 sec)	-0.69	-0.47	1.24	-1.12	-1.04	-0.59	-0.61	0.54	-1.19	-0.92	-1.13	-0.80	-0.33	-0.80	0.74	-0.28	-0.53	-0.89	0.61	0.55	0.43	0.73	0.03	0.02

	ER1A	ER1B	ER2A	ER3A	3NW3	3NW4	3NW5	3NW6	3NW7	5NW3	5NW7	3EW1	3EW3	3EW1	3SW1	3SW2	3SW3	3SW4	3NW1	3NW2
\bar{p} (N/m ²)	16	-43	-22	-5	21	22	18	5	-8	-23	10	-41	-40	-44	-50	-60	-52	-42	5	-48
σ_p (N/m ²)	7	21	17	-	24	22	24	23	20	31	25	19	16	18	23	26	21	20	21	32
P max (N/m ²)	65	17	49	194	149	143	170	144	120	136	195	12	3	15	27	32	395	21	431	43
P min (N/m ²)	-6	-181	-221	-16	-51	-39	-62	-66	-101	-115	-76	-140	-118	-131	-272	-283	-153	-179	-96	-274
g	7.0	6.1	11.7	-	5.3	5.5	6.3	5.3	6.4	5.1	7.4	5.2	4.9	4.8	9.6	8.6	-	6.9	-	7.1
C \bar{p}	0.19	-0.50	-0.26	-0.06	0.24	0.26	0.21	0.06	-0.09	-0.27	0.12	-0.48	-0.46	-0.51	-0.58	-0.70	-0.60	-0.49	0.06	-0.56
C \hat{p} (2 sec)	0.17	-0.48	-0.39	0	0.54	0.49	0.48	0.33	0.20	0.44	0.40	-0.51	-0.43	-0.51	-0.63	-0.69	-0.01	-0.52	0.25	-0.71
C \hat{p} (1/32 sec)	0.30	-0.85	-1.04	0.61	0.70	0.67	0.80	0.68	0.57	0.64	0.92	-0.65	-0.65	-0.62	-1.28	-1.33	1.85	-0.84	-	-1.29

Duration 1024 seconds; u_{10} 11.9 m/s; u_5 7.5 m/s; u_3 6.2 m/s; u_{10} 18.6 m/s; u_5 14.1 m/s; u_3 14.7 m/s; β 235°; θ 285°.

Table 6 Record A12A

	WR1A	WR1C	WR1D	WR1E	WR3A	WR3B	WR3C	WR3E	WR4A	WR4E	SW1	SW2	SW4
\bar{p} (N/m ²)	-31	-109	-36	-23	-31	-21	-17	-16	-40	-57	-16	-11	-12
σ_p (N/m ²)	16	41	14	9	16	6	5	6	24	20	24	26	7
P max (N/m ²)	12	112	142	-2	-5	19	39	61	-1	-12	113	73	21
P min (N/m ²)	-169	-276	-112	-90	-144	-80	-55	-64	-202	-185	-148	-163	-53
g	13.5	5.8	15.4	10.7	7.5	11.2	13.2	16.3	7.7	7.8	5.9	6.2	6
$C_{\bar{p}}$	-0.7	-2.5	-0.83	-0.53	-0.71	-0.48	-0.39	-0.37	-0.92	-1.31	-0.37	-0.25	-0.28
$C_{\bar{p}}$ (2 sec)	-0.72	-1.58	-0.07	-0.45	-0.74	-0.28	-0.24	-0.28	-0.93	-0.85	-0.58	-0.63	-0.23
$C_{\bar{p}}$ (1/32 sec)	-1.13	-1.84	0.94	-0.80	-0.96	-0.53	-0.36	-0.43	-1.35	-1.23	-0.99	-1.09	-0.35

	ER1A	ER1B	ER2A	ER3A	ER3B	3VW2	3VW4	3VW5	3VW6	3VW7	5VW3	5VW7
\bar{p} (N/m ²)	-29	-19	-54	-57	-63	15	18	24	25	19	11	32
σ_p (N/m ²)	10	7	20	27	25	14	15	18	17	13	16	21
P max (N/m ²)	7	41	61	127	4	96	138	103	89	72	117	142
P min (N/m ²)	-107	-58	-135	-175	-192	-26	-39	-27	-33	-84	-37	-102
g	6.9	8.9	0.0	6.8	5.2	5.8	8.0	-1.4	3.8	7.9	6.6	6.4
$C_{\bar{p}}$	-0.87	-0.44	-1.24	-1.31	-1.44	0.34	0.41	0.55	0.57	0.44	0.25	0.73
$C_{\bar{p}}$ (2 sec)	-0.41	-0.27	-0.89	-0.98	-0.98	0.54	0.02	0.60	0.56	-0.13	0.54	0.67
$C_{\bar{p}}$ (1/32 sec)	-0.71	-0.38	-0.90	-1.17	-1.28	0.64	0.92	0.68	0.59	-0.56	0.78	0.95

Duration 1024 seconds; \bar{u}_{10} 8.4 m/s; \bar{u}_3 7.4 m/s; \hat{u}_{10} 15.6 m/s; \hat{u}_3 13.7 m/s; β 205°; θ 235°.

Table 7 Record A12B

	WR1A	WR1C	WR1D	WR1E	WR3A	WR3B	WR3C	WR3E	WR4A	WR4E	3SW1	3SW2	3SW4
\bar{p} (N/m ²)	-20	-78	-28	-15	-24	-19	-14	-12	-33	-52	-12	-8	-11
σ_p (N/m ²)	11	24	11	7	16	5	4	4	22	17	23	25	7
P_{max} (N/m ²)	27	74	50	9	13	7	22	28	11	1	122	130	39
P_{min} (N/m ²)	-87	-263	-94	-47	-12	-41	-30	-32	-206	-132	-130	-138	-85
g	6.1	5.4	7.1	4.6	2.3	4.4	9	10	7.9	4.7	5.8	5.5	12
$C_{\bar{p}}$	-0.46	-1.81	-0.65	-0.35	-0.56	-0.44	-0.33	-0.28	-0.77	-1.21	-0.28	-0.19	-0.26
$C_{\hat{p}}$ (2 sec)	-0.39	-1.47	-0.52	-0.25	-0.74	-0.28	-0.20	-0.17	-0.93	-0.83	-0.51	-0.63	-0.24
$C_{\hat{p}}$ (1/32 sec)	-0.65	-1.97	-0.71	-0.35	-0.93	-0.31	-0.22	-0.24	-1.54	-0.98	-0.99	-1.03	-0.71

	ER1A	ER1B	ER2A	ER3A	3WW3	3WW4	3WW5	3WW6	3WW7	5WW3	5WW7	ER3B
\bar{p} (N/m ²)	-31	-21	-58	-72	14	15	21	23	17	13	30	-63
σ_p (N/m ²)	11	7	20	30	13	14	18	18	14	14	23	22
P_{max} (N/m ²)	1	9	61	127	81	102	133	134	66	241	168	4
P_{min} (N/m ²)	-107	-58	-135	-174	-59	-40	-27	-18	-66	-24	-46	-178
g	6.9	5.3	5.0	6.6	5.6	6.2	6.2	6.2	5.9	16.3	6.0	5.2
$C_{\bar{p}}$	-0.72	-0.49	-1.35	-1.68	0.33	0.35	0.49	0.54	0.40	0.30	0.70	-1.47
$C_{\hat{p}}$ (2 sec)	-0.50	-0.33	-0.91	-1.1	0.46	0.58	0.80	0.75	0.41	0.50	0.77	-1.07
$C_{\hat{p}}$ (1/32 sec)	-0.80	-0.44	-1.01	-1.3	0.61	0.77	0.99	1.0	0.50	1.80	1.25	-1.33

Duration 1024 seconds; \bar{u}_{10} 8.4 m/s; \bar{u}_3 7.3 m/s; \hat{u}_{10} 14.7 m/s; \hat{u}_3 12.9 m/s; $\bar{\theta}$ 205°; $\hat{\theta}$ 235°.

Table 12 Comparison of various methods of calculating pressure coefficients; transducer WR1C

Record no	Roof pitch	Ridge height h (m)	\bar{p} (N/m ²)	\hat{p} (N/m ²)	$C_{\bar{p}}$ based on:		$C_{\hat{p}}$ based on:			
					\bar{q}_{10}	\bar{q}_h	\bar{q}_{10}	\bar{q}_h	\hat{q}_{10}	\hat{q}_h
A12A	10°	5.9	- 109	- 276	- 2.5	- 2.9	- 6.3	- 7.3	- 1.8	- 2.1
A12B	15°	6.2	- 78	- 253	- 1.8	- 2.1	- 6.1	- 7.0	- 2.0	- 2.3
A11	22½°	6.8	- 44	- 255	- 0.8	- 0.9	- 4.7	- 5.2	- 1.0	- 1.2

\hat{p} is 1/32 second value; \hat{q}_{10} and \hat{q}_h are 2 second values.

\bar{q}_h and \hat{q}_h were interpolated linearly from the values of \bar{q}_{10} and \bar{q}_3 , and of \hat{q}_{10} and \hat{q}_3 respectively.

Table 8 Record A25B

	3NW7	3NW2	3NW5	3NW4	3NW5	3NW6	3NW7	3NW7	3NW2	3NW3	3NW4	3NW5	3NW6	3NW7	3EW1	3EW2	3EW3
\bar{p} (N/m ²)	11	14	7	13	8	4	-6	22	26	24	25	23	16	7	-22	-20	-20
σ_p (N/m ²)	14	13	11	13	11	12	11	17	17	14	15	14	13	11	8	7	7
p_{max} (N/m ²)	91	62	66	86	74	81	64	102	98	93	102	94	102	72	-3	-4	-5
p_{min} (N/m ²)	-20	-30	-18	-18	-20	-42	-67	-15	-29	-6	-7	-14	-18	-51	-66	-42	-41
g	5.7	3.6	5.2	5.7	6.3	6.4	5.9	4.7	4.2	4.7	5.1	5.0	6.5	5.8	5.1	3.3	3.2
$C_{\bar{p}}$	0.26	0.31	0.17	0.29	0.19	0.08	-0.13	0.50	0.59	0.55	0.58	0.53	0.37	0.17	-0.51	-0.45	-0.46
$C_{\bar{p}}$ (2 sec)	0.53	0.46	0.45	0.60	0.46	0.52	0.34	0.69	0.67	0.64	0.67	0.63	0.53	0.41	-0.43	-0.40	-0.38
$C_{\bar{p}}$ (1/32 sec)	0.90	0.61	0.65	0.85	0.73	0.80	-0.66	1.00	0.96	0.91	1.01	0.89	1.00	0.71	-0.65	-0.41	-0.41

	3EW3	3EW5	3EW7	3EW2	3EW3	3EW4	3EW5	3SW1	3SW2	3SW3	3SW4	3SW7	3SW2	3NW1	3NW2	INT
\bar{p} (N/m ²)	-27	-19	-18	-17	-19	-19	-20	-32	-34	-33	-25	-30	-32	-19	-29	-16
σ_p (N/m ²)	9	7	7	6	7	7	7	10	12	11	10	11	12	10	15	-
p_{max} (N/m ²)	-6	-2	-2	-2	-3	-1	2	-6	-1	1	3	3	1	13	35	-
p_{min} (N/m ²)	-59	-47	-42	-39	-42	-42	-46	-101	-105	-77	-71	-78	-86	-68	-95	-
g	3.7	4.2	3.5	3.4	3.5	3.5	3.8	6.6	6.2	3.5	4.4	4.4	4.4	4.8	4.4	-
$C_{\bar{p}}$	-0.61	-0.45	-0.41	-0.40	-0.42	-0.44	-0.46	-0.73	-0.79	-0.76	-0.58	-0.69	-0.74	-0.45	-0.86	-
$C_{\bar{p}}$ (2 sec)	-0.53	-0.39	-0.34	-0.36	-0.36	-0.36	-0.38	-0.65	-0.61	-0.69	-0.52	-0.60	-0.64	-0.44	-0.69	-
$C_{\bar{p}}$ (1/32 sec)	-0.58	-0.46	-0.41	-0.38	-0.41	-0.42	-0.45	-0.99	-1.04	-0.76	-0.70	-0.77	-0.89	-0.67	-0.93	-

Duration 512 seconds; \bar{u}_{10} 8.4 m/s; \bar{u}_5 6.5 m/s; \bar{u}_3 5.4 m/s; \hat{u}_{10} 12.9 m/s; \hat{u}_5 12.4 m/s; \hat{u}_3 11.2 m/s; $\bar{\beta}$ 250°; $\bar{\theta}$ 280°.

Table 9 Record A29

	3WW1	3WW2	3WW3	3WW4	3WW5	3WW6	3WW7	5WW1	5WW2	5WW3	5WW4	5WW5	5WW6	5WW7	3EW1	3EW2
\bar{p} (N/m ²)	-33	-22	-11	-7	-2	-6	-6	-27	-17	-6	-3	-2	-4	-5	-9	-7
σ_p (N/m ²)	15	14	8	7	5	4	3	12	14	9	8	6	4	3	5	6
P_{max} (N/m ²)	22	16	14	16	14	10	7	23	27	21	20	19	12	7	9	11
P_{min} (N/m ²)	-116	-90	-45	-40	-25	-31	-23	-91	-86	-58	-51	-42	-38	-36	-43	-47
g	5.7	4.8	4.3	4.8	5.0	6.5	5.0	5.5	5.0	5.6	6.3	7.1	8.6	9.0	6.9	6.6
$C_{\bar{p}}$	-0.74	-0.49	-0.25	-0.15	-0.06	-0.13	-0.13	-0.60	-0.37	-0.13	-0.06	-0.04	-0.08	-0.11	-0.20	-0.17
$C_{\hat{p}}$ (2 sec)	-0.83	-0.67	-0.36	-0.27	-0.15	-0.17	-0.16	-0.73	-0.63	-0.36	-0.30	-0.17	-0.17	-0.16	-0.34	-0.35
$C_{\hat{p}}$ (1/32 sec)	-1.09	-0.84	-0.42	-0.37	-0.23	-0.29	-0.21	-0.85	-0.80	-0.54	-0.47	-0.40	-0.36	-0.33	-0.40	-0.44

	3EW3	3EW4	3EW5	5EW1	5EW2	5EW3	5EW4	5EW5	3SW1	3SW2	3SW3	3SW4	5SW1	5SW2	3NW1	3NW2
\bar{p} (N/m ²)	-14	-28	-35	-7	-7	-13	-25	-29	-12	-10	-7	-9	-8	-7	18	25
σ_p (N/m ²)	10	13	12	5	8	11	13	11	4	4	4	4	3	3	11	12
P_{max} (N/m ²)	14	14	5	10	14	19	20	0	0	1	4	3	3	2	-8	-2
P_{min} (N/m ²)	-54	-92	-97	-45	-64	-67	-92	-86	-27	-26	-26	-33	-24	-23	71	75
g	4.2	5.0	5.1	7.2	7.2	4.7	5.1	5.3	4.0	4.8	5.0	6.0	5.4	5.4	4.9	4.2
$C_{\bar{p}}$	-0.30	-0.62	-0.76	-0.15	-0.17	-0.28	-0.55	-0.65	-0.27	-0.21	-0.17	-0.20	-0.17	-0.16	0.39	0.56
$C_{\hat{p}}$ (2 sec)	-0.41	-0.75	-0.78	-0.30	-0.34	-0.44	-0.67	-0.71	-0.21	-0.20	-0.23	-0.27	-0.16	-0.17	0.56	0.64
$C_{\hat{p}}$ (1/32 sec)	-0.51	-0.86	-0.91	-0.42	-0.60	-0.62	-0.86	-0.80	-0.25	-0.25	-0.24	-0.31	-0.22	-0.21	0.67	0.70

Duration 1024 seconds; $\bar{u}_{10} = 8.6$ m/s; $\bar{u}_5 = 6.3$ m/s; $\bar{u}_3 = 5.2$ m/s; $\hat{u}_{10} = 13.2$ m/s; $\hat{u}_5 = 9.8$ m/s; $\hat{u}_3 = 9.8$ m/s; $\bar{\theta} = 330^\circ$; $\bar{\theta} = 0^\circ$.

Table 10 Record A31B

	3WW1	3WW2	3WW3	3WW4	3WW5	3WW6	3WW7	5WW1	5WW2	5WW3	5WW4	5WW5	5WW6	5WW7	5EW1	5EW2	5EW3
\bar{p} (N/m ²)	0	-1	-21	-40	-45	-45	-52	12	29	15	-1	-16	-18	-19	-52	-50	-17
σ_p (N/m ²)	11	13	20	27	26	19	23	18	18	21	25	19	15	14	28	29	19
P_{max} (N/m ²)	44	46	40	38	37	15	14	91	96	99	112	77	45	33	27	30	46
P_{min} (N/m ²)	-63	-69	-100	-147	-191	-162	-227	-18	-72	-79	-115	-112	-107	-102	-263	-188	-107
g	6.0	5.1	4.0	4.0	5.7	6.3	7.8	4.9	3.8	4.1	4.5	5.1	5.8	6.2	8.3	4.8	4.8
$C_{\bar{p}}$	0	-0.01	-0.20	-0.37	-0.41	-0.41	-0.48	0.11	0.27	0.14	0	-0.14	-0.17	-0.17	-0.48	-0.46	-0.16
$C_{\hat{p}}$ (2 sec)	-0.11	-0.15	-0.29	-0.42	-0.39	-0.39	-0.53	0.27	0.29	0.30	-0.19	-0.22	-0.23	-0.23	-0.61	-0.55	-0.29
$C_{\hat{p}}$ (1/32 sec)	-0.23	-0.25	-0.36	-0.53	-0.69	-0.59	-0.82	0.33	0.35	0.36	-0.42	-0.40	-0.39	-0.37	-0.95	-0.87	-0.38

	3EW4	3EW5	5EW1	5EW2	5EW3	5EW4	5EW5	3SN1	3SN2	3SN3	3SN4	5SN1	5SN2	3NW1	3NW2	INT
\bar{p} (N/m ²)	-6	-6	-31	-43	-13	-4	-5	28	39	57	49	31	82	-9	-10	48
σ_p (N/m ²)	14	9	17	25	23	16	11	20	26	27	27	37	34	7	8	-
P_{max} (N/m ²)	50	40	36	36	63	42	29	133	154	176	176	203	222	15	15	-
P_{min} (N/m ²)	-97	-72	-139	-169	-137	-108	-97	-25	-15	1	-5	-44	16	-34	-42	-
g	6.6	7.1	6.2	5.0	5.4	6.5	8.7	5.1	4.5	4.3	4.7	4.7	4.1	3.8	4.1	-
$C_{\bar{p}}$	-0.6	-0.06	-0.29	-0.40	-0.12	-0.03	-0.04	0.26	0.36	0.53	0.46	0.29	0.76	-0.08	-0.10	-
$C_{\hat{p}}$ (2 sec)	-0.23	-0.16	-0.36	-0.41	-0.33	-0.25	-0.18	0.36	0.47	0.58	0.53	0.54	0.72	-0.11	-0.12	-
$C_{\hat{p}}$ (1/32 sec)	-0.35	-0.26	-0.50	-0.61	-0.49	-0.39	-0.35	0.48	0.56	0.63	0.63	0.73	0.80	-0.12	-0.15	-

Duration 1024 seconds; \bar{u}_{10} 13.3 m/s; \bar{u}_5 11.8 m/s; \bar{u}_3 10.8 m/s; \hat{u}_{10} 21.2 m/s; \hat{u}_5 19.8 m/s; \hat{u}_3 18.6 m/s; $\bar{\beta}$ 150°; $\bar{\theta}$ -180°.

Table 10 Record A31B (continued)

	WR1A	WR1B	WR1C	WR1D	WR1E	WR1F	WR3A	WR3B	WR3D	WR4A	WR4E	ER1A	ER1B	ER1C	ER2A	ER2C	ER3A
\bar{p} (N/m ²)	-59	-47	-23	-5	26	39	-27	-27	20	-5	79	-90	-7	-9	-12	39	0
σ_p (N/m ²)	31	25	25	20	18	13	19	18	21	2	56	42	17	7	3	19	2
P_{max} (N/m ²)	9	31	73	77	102	91	14	78	115	1	135	-6	62	19	5	113	6
P_{min} (N/m ²)	-252	-202	-169	-108	-57	-5	-203	-156	-62	-16	-68	-306	-112	-49	-28	-10	-17
g	6.2	6.2	5.9	5.1	4.2	4.1	9.2	7.0	4.4	8.7	1.0	5.2	8.1	5.8	4.6	4.0	7.1
$C_{\bar{p}}$	-0.54	-0.43	-0.21	-0.05	0.24	0.36	-0.25	-0.25	-0.18	-0.03	0.73	-0.83	-0.06	-0.08	-0.11	0.36	0
$C_{\bar{p}}$ (2 sec)	-0.70	-0.55	-0.36	-0.21	0.29	0.33	-0.45	-0.34	0.33	-0.04	0.36	-0.90	-0.21	-0.11	-0.07	0.33	-0.03
$C_{\bar{p}}$ (1/32 sec)	-0.91	-0.73	-0.61	-0.39	0.37	0.28	-0.74	-0.56	0.42	-0.06	0.49	-1.11	-0.40	-0.18	-0.10	0.41	-0.06

Duration 1024 seconds; \bar{u}_{10} - 13.3 m/s; \bar{u}_5 - 11.8 m/s; \bar{u}_3 - 10.8 m/s; \hat{u}_{10} - 21.2 m/s; \hat{u}_5 - 19.8 m/s; \hat{u}_3 - 18.6 m/s; $\bar{\beta}$ - 150°; $\bar{\theta}$ - 180°.

Table 11 Record A32

	3WW1	3WW2	3WW3	3WW4	3WW5	3WW6	3WW7	5WW1	5WW2	5WW3	5WW4	5WW5	5WW6	5WW7	3EW1	3EW2	3EW3
\bar{p} (N/m ²)	11	28	36	37	36	-	-	42	64	62	67	63	58	43	-54	-59	-58
σ_p (N/m ²)	32	32	31	36	33	-	-	39	41	38	42	40	38	35	21	21	20
P_{max} (N/m ²)	197	216	247	229	214	-	-	264	283	256	279	280	284	223	-8	-11	-1
P_{min} (N/m ²)	-59	-41	-48	-48	-39	-	-	-48	-31	-20	-22	-22	-29	-46	-205	-165	-167
g	5.8	6.0	6.9	5.4	5.3	-	-	5.7	5.4	5.1	5.1	5.5	5.9	5.1	7.2	4.9	5.5
$C_{\bar{p}}$	0.09	0.21	0.29	0.29	0.29	-	-	0.34	0.51	0.50	0.54	0.51	0.46	0.35	-0.43	-0.48	-0.47
$C_{\bar{p}}$ (2 sec)	0.35	0.40	0.50	0.50	0.48	-	-	0.48	0.62	0.54	0.65	0.69	0.59	0.45	-0.49	-0.41	-0.41
$C_{\bar{p}}$ (1/32 sec)	0.54	0.59	0.68	0.63	0.59	-	-	0.72	0.77	0.70	0.76	0.76	0.77	0.61	-0.56	-0.45	-0.46

Duration 1024 seconds; \bar{u}_{10} - 14.3 m/s; \bar{u}_5 - 11.7 m/s; \bar{u}_3 - 10.2 m/s; \hat{u}_{10} - 24.4 m/s; \hat{u}_5 - 20.4 m/s; \hat{u}_3 - 19.5 m/s; $\bar{\beta}$ - 235°; $\bar{\theta}$ - 265°.

(Continued on page 36)

Table 11 Record A32 (continued)

	3EW4	3EW5	5EW1	5EW2	5EW3	5EW4	5EW5	3SW1	3SW2	3SW3	3SW4	5SW1	5SW2	3NW1	3NW2	INT
\bar{p} (N/m ²)	-67	-66	-46	-49	-53	-58	-61	-61	-91	-64	-35	-97	-93	-82	-94	-59
σ_p (N/m ²)	23	23	18	18	20	20	24	41	46	33	20	54	56	32	37	-
P max (N/m ²)	-14	-8	-7	-8	-5	-11	-7	124	70	32	24	158	102	14	9	-
P min (N/m ²)	-165	-166	-140	-144	-156	-148	-168	-280	-353	-245	-149	-348	-360	-231	-260	-
G	4.3	4.3	5.2	5.1	5.3	4.4	4.4	5.4	5.7	5.4	5.8	4.7	4.7	4.7	4.5	-
C \bar{p}	-0.54	-0.53	-0.37	-0.39	-0.42	-0.47	-0.52	-0.49	-0.73	-0.51	-0.28	-0.78	-0.74	-0.66	-0.76	-
C \bar{p} (2 sec)	-0.39	-0.38	-0.36	-0.37	-0.39	-0.35	-0.38	-0.57	-0.74	-0.50	-0.30	-0.85	-0.84	-0.52	-0.57	-
C \bar{p} (1/32 sec)	-0.45	-0.45	-0.38	-0.39	-0.43	-0.40	-0.46	-0.77	-0.96	-0.67	-0.41	-0.95	-0.59	-0.63	-0.71	-

	WR1A	WR1B	WR1C	WR1D	WR1E	WR1F	WR3A	WR3B	WR3C	WR3D	WR4A	WR4E	ER1A	ER1B	ER1C	ER2A	ER2C	ER3A
\bar{p} (N/m ²)	-25	-43	-25	-28	-33	-52	-13	-3	3	-10	-6	-15	-69	-78	-72	24	-47	-20
σ_p (N/m ²)	26	31	30	29	34	31	9	8	3	12	1	13	26	31	26	3	20	26
P max (N/m ²)	85	85	93	82	110	72	50	54	16	58	-2	47	-13	11	-19	43	1	21
P min (N/m ²)	-166	-212	-174	-192	-212	-207	-98	-51	-12	-68	-16	-78	-202	-245	-231	9	-200	-282
G	5.3	5.5	5.0	5.7	5.3	5.0	0.2	5.6	4.41	4.7	7.6	4.9	5.2	5.3	6.2	5.4	7.6	10.0
C \bar{p}	-0.20	-0.34	-0.20	-0.22	-0.26	-0.42	-0.10	-0.03	0.02	-0.08	-0.05	-0.12	-0.56	-0.63	-0.58	0.20	-0.38	-0.16
C \bar{p} (2 sec)	-0.31	-0.38	-0.33	-0.41	-0.39	-0.34	-0.16	0.07	0.03	-0.10	-0.03	-0.14	-0.47	-0.49	-0.48	0.10	-0.38	-0.59
C \bar{p} (1/32 sec)	-0.45	-0.58	-0.48	0.52	-0.58	-0.57	-0.27	0.15	0.04	-0.19	-0.04	-0.21	-0.55	-0.67	-0.63	0.12	-0.55	-0.77

Duration 1024 seconds; \bar{u}_{10} 14.3 m/s; \bar{u}_5 11.7 m/s; \bar{u}_3 10.2 m/s; \hat{u}_{10} 24.4 m/s; \hat{u}_5 20.4 m/s; \hat{u}_3 19.5 m/s; $\bar{\theta}$ 235°; $\hat{\theta}$ 265°.